UNIVERSITY OF INSUBRIA

DEPARTMENT OF CLINICAL AND EXPERIMENTAL MEDICINE

ARRAY COMPARATIVE GENOMIC HYBRIDIZATION ANALYSIS OF OLFACTORY NEUROBLASTOMA

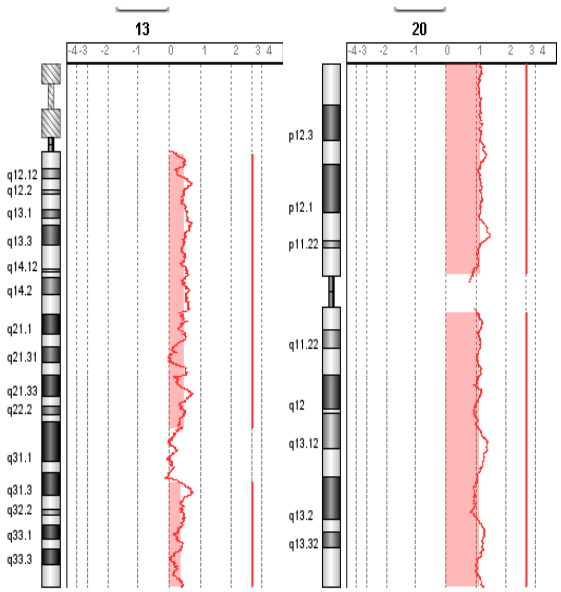

Dr Francesca De Bernardi

Tutor: prof. Maserati
Supervisor: prof. Pasquali

PhD School in Biological and Medical Sciences
PhD Program in “Experimental Medicine and Oncology”
XXIII Cycle

CONTENTS

FIGURES INDEX

TABLES INDEX

1. INTRODUCTION

The olfactory neuroblastoma (ONB) is an uncommon malignant neoplasm arising from the olfactory epithelium (Rinaldo 2002, Dulguerov 2001). It represents 3% of malignant tumours of the nasal cavity and paranasal sinuses (Bradley 2003, Broich 1997) with an estimated incidence of 0.4 patients per million per year. Given the low incidence of this disease, the clinical features and survival data are difficult to analyze. The Department of Otolaryngology Hospital of Varese is a tertiary-care referral unit for the endoscopic treatment of skull base tumours. From 1997 to 2011, 213 patients with skull base tumours were treated at this hospital and among these 21 patients with ONB.

The behavior of these tumours varies greatly: some patients survive with the disease for more than 20 years, whereas in others, survival is limited to few months due to catastrophic progression and dissemination (Bradley 2003). The overall survival of this tumour at 5 years is 62.1%, and 10 years is 45.6% (Jethanamest 2007).

The traditional grading's system according to Hyams is based on several tumour histological parameters (architecture, pleomorphism, neurofibrillary matrix, rosettes, mitosis, necrosis), Grades I being well differentiated to IV undifferentiated, and has a good correlation with survival. Patients with low-grade olfactory neuroblastoma have a better prognosis with a survival that exceeds 20 years (1 and 56% grade II), while in cases of high-grade, the progression of the disease can be very fast, with survival limited to a few months (25% grade III-IV) (Bradley 2003).

The divergence of the clinical behavior requires a better characterization of patients with worse prognosis. So there has been a review of case studies with the collaboration of pathological anatomy, which has allowed a careful re-evaluation of morphological and immunophenotypic features. Immunohistochemical studies using antibodies against the use of tissue specific markers allow to better characterize the ONB. In particular, it allows the differential diagnosis between high-grade ONB according to Hyams and neuroendocrine carcinoma (NEC), which most frequently enters into differential diagnosis with this disease.

Moreover, thanks to the cooperation with the Division of Biology and Medical Genetics, Department of Clinical and Experimental Medicine, it was possible to perform a study of molecular biology. The molecular studies are extremely limited and are aimed at identifying the genetic profile correlated with a worse prognosis.

Therefore, the aim of our study is to analyze the genetic profile of ONB with competitive genomic hybridization (array comparative genomic hybridization – a-CGH) and to correlate this profile with the clinical evolution and to compare our data with literature.

The analyzed patients were treated at the Department of Otolaryngology of Varese and followed with a careful follow-up for a period of about 10 years. At the Department of Pathology tumour samples of the patients were reviewed with the use of new immunohistochemical techniques. At the Section of Biology and Medical Genetics, Department of Clinical and Experimental medicine, the DNA analysis of tumour patients were carried out using a-CGH techniques.

2. OLFACTORY NEUROBLASTOMA

Olfactory neuroblastoma (ONB) is an uncomm malignant neuroectodermal nasal tumour. ONBs are thought to arise from the specialized sensory neuroepithelial (neuroectodermal) olfactory cells that are normally found in the upper part of the nasal cavity, including the superior nasal concha, the upper part of septum, the roof of nose, and the cribriform plate of ethmoid (Thompson LD 2009).

2.1 Clinical features

The incidence of olfactory neuroblastoma was found 0.4 cases/million inhabitants per year. The incidence of olfactory neuroblastoma is difficult to establish, but the tumour is not as rare as is commonly reported and probably represents more than 5% of all nasal malignant tumours (Lund 2010).

ONB may occur at any age (2–94 years), but a bimodal age distribution in the 2nd and 6th decades of life are most common without a gender predilection. Occasional cases have also been reported in children. Olfactory neuroblastoma affects male and female patients with similar frequency and can be found in all age groups (Dulguerov 1992).

The tumours most commonly cause unilateral nasal obstruction (70%), and epistaxis (50%), while less common signs and symptoms include headaches, pain, excessive lacrimation, rhinorrhea, anosmia, and visual disturbances. Even though the tumour arises from the olfactory neuroepithelium, anosmia is not a common complaint (5%). Due to the non-specific nature of the initial presentation and slow growth of the tumours, patients often have a long history before diagnosis (Thompson LD 2009, Davis RE 1992, Eden BV 1994, Resto VA 2000).

Palpable cervical nodes may be present at diagnosis. According to Levine et al. (Levine 1999), the rate of patients with nodal metastasis increases from 6% to 25% when the entire clinical history of patients is considered. These data are in keeping with those from Rinaldo et al. (Rinaldo 2002) and Ferlito et al. (Ferlito 2003), who extensively reviewed the literature and found an overall rate of lymph node metastases (synchronous and metachronous) from olfactory neuroblastoma of

approximately 23%.

At endoscopy, olfactory neuroblastoma appears as a broad-based, highly vascularized mass, with polypoid appearance. It usually has an irregular, lobulated surface and a color varying from gray to red (Walch et al. 2000). Particularly in the early stages, the mass is typically confined to the olfactory cleft, but more advanced lesions frequently extend through the upper part of the nasal septum to involve both nasal fossae.

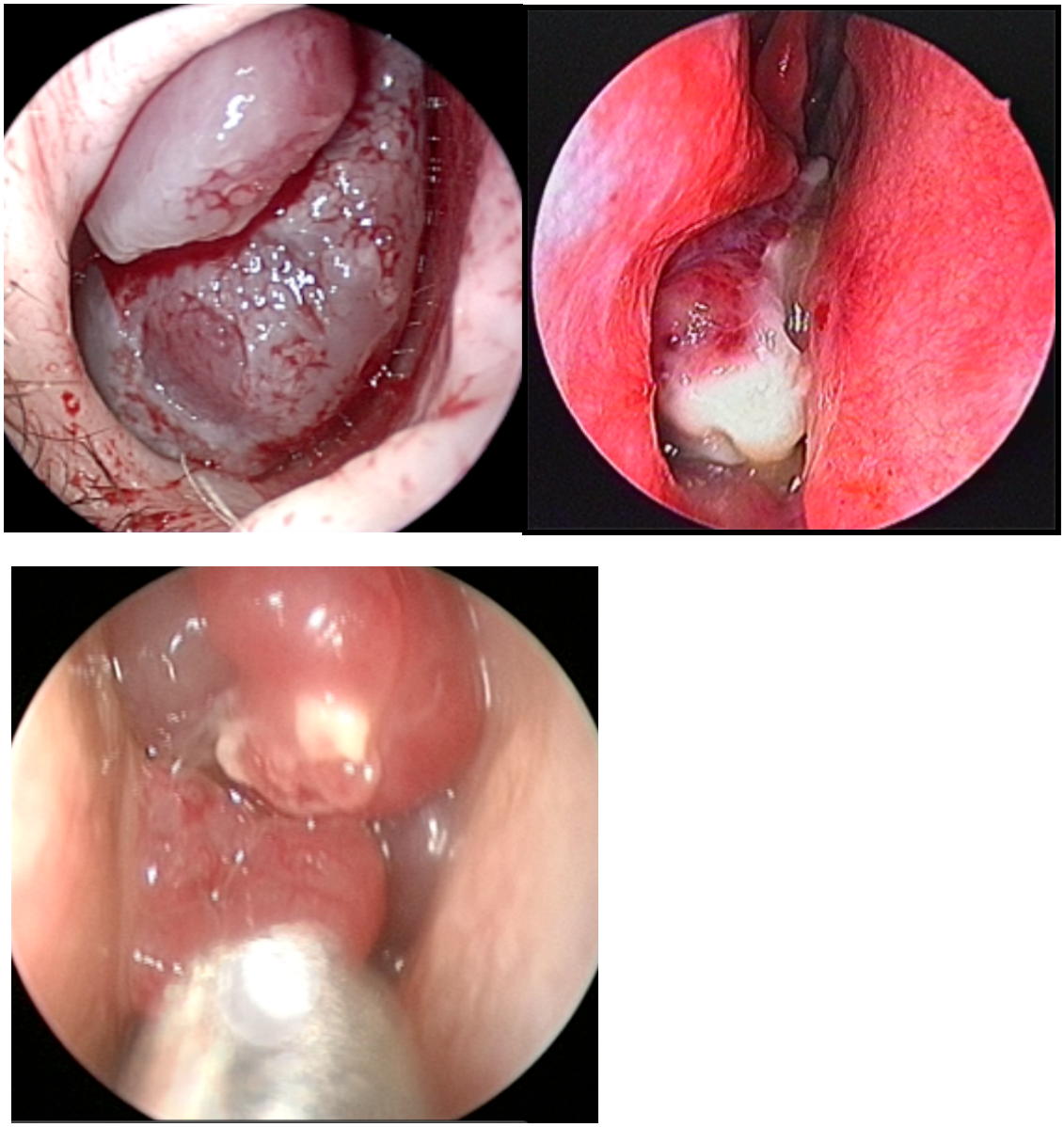

Figure 1: Endoscopic view of olfactory neuroblastoma

2.2 Imaging Studies

The imaging features of olfactory neuroblastoma are nonspecific. Nevertheless, this neoplasm should be suspected when a mass is detected in the superior nasal cavity, causing either remodeling or destruction of adjacent bony structures, and erosion of the cribriform plate or of the fovea ethmoidalis (Som et al. 1994; Woodhead and Lloyd 1988; Jiang GY et al. 2011; Derdeyn et al. 1994; Schuster et al. 1994; Pickuth et al. 1999).

In fact, because olfactory neuroblastoma arises from the olfactory epithelium, most cases have the epicenter in the uppermost nasal cavity or in the adjacent ethmoid cells.

At an early stage, olfactory neuroblastoma can be totally confined within the nasal cavity or the ethmoid, without contacting the roof.

At an advanced stage a “dumbbell-shaped” mass extending across the cribriform plate is one of the most characteristic imaging findings for this tumour. The upper portion is a mass in the intracranial fossa, while the lower portion is in the nasal cavity, with the “waist” at the cribriform plate.

CT will show speckled calcifications and bone erosion of the lamina papyracea, cribriform plate and/or the fovea ethmoidalis by non-contrast methods. Contrast enhanced CT will show homogenously enhancing mass, with non-enhancing areas suggesting regions of necrosis.

Absence of changes of the bony interface on CT does not reliably exclude subtle intracranial spread. MR is ideally suited for this, because it shows even small neoplastic projections that travel through the sieve-like openings across the fenestrations of the cribriform plate, whereas positivity on CT requires bone destruction (Li et al. 1993).

MRI images with and without contrast will delineate the extent of the disease, with T1-weighted images showing hypointense-to-intermediate signal intensity within the mass compared to the brain, while areas of necrosis will be hypointense. T2-weighted images may show hyperintense regions which correlate to the cystic regions at the advancing edge (Kareimo KJA et al. 1998). There is often marked tumour enhancement after gadolinium. ONB may rarely present with only an intracranial (frontal lobe) mass. Ectopic tumours within the paranasal sinuses (not ethmoid) are

vanishingly rare, except in recurrent tumours (Thompson LD 2009). Due to its high vascularization, olfactory neuro- blastoma shows either homogeneous or heteroge- neous intense enhancement (Schuster et al. 1994). Actually, a dense blush is detectable on angiography.

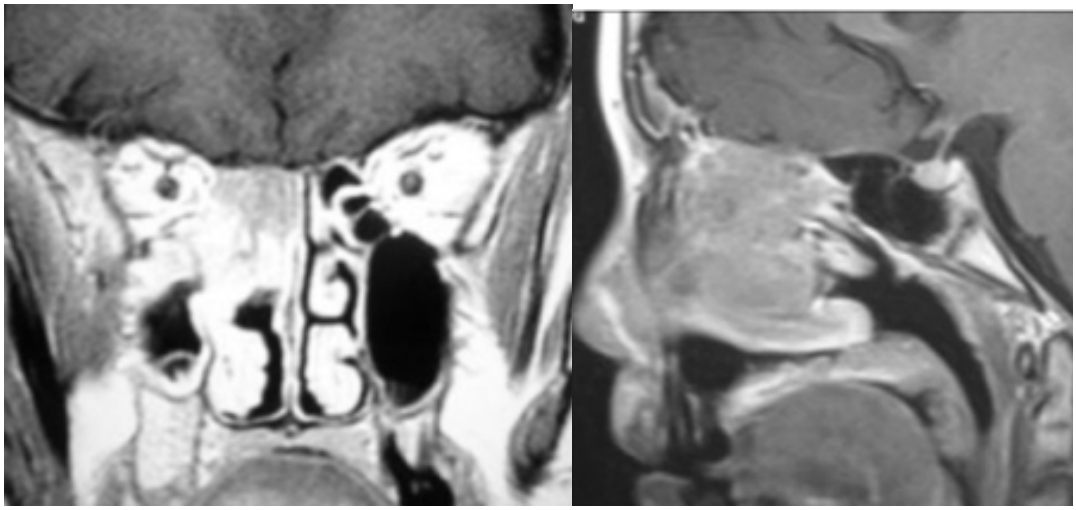

a b

c

Figure 2: RM aspects of ONB

a Coronal MR T1 with contrast shows a mass with a low- to intermediate signal and its epicenter within the right ethmoid, **b** On sagittal plane MR demonstrates that the tumor does not extend into the anterior cranial fossa **c** A post contrast sagittal MR of a case with intracranial spread into the anterior cranial fossa

2.3 Staging system

Different staging systems based on the extension of the lesion (Kadish et al. 1976; Dulguerov and Calcaterra 1992) have been specifically proposed for olfactory neuroblastoma (Table 1 and 2).

Table 1: Kadish staging system

Kadish staging system (1976)

Stage Features
A Tumour confined to the nasal cavity
B Tumour confined to the nasal cavity, involving one or more paranasal sinuses
C Tumour extending beyond the nasal cavity and parana- sal sinuses. Includes involving of the orbit, skull base, intracranial cavity, cervical lymph nodes and distant metastatic sites

Table 2: Dulguerov and Calcaterra staging system

Dulguerov and Calcaterra staging system (1992)

Stage Features
T1 Tumour involving the nasal cavity and/or paranasal sinuses, sparing the most superior ethmoidal cells
T2 Tumour involving the nasal cavity and/or paranasal sinuses, including the sphenoid, with extension to and erosion of the cribriform plate
T3 Tumour extending into the orbit or protruding into the anterior cranial fossa
T4 Tumour involving the brain

Most curious for modern staging systems, the Kadish et al. proposed staging system from 1976 is still used. The main source of criticism towards Kadish classification is that it groups together in the C category situations with a different impact on prognosis as, for example, skull base involvement and widespread disease. Dulguerov and Calcaterra (1992) provided a more reliable prognostic stratification of patients, by creating a T4 category for patients with brain involvement. However, their staging system is strictly focused on the local extent of the tumour and does not take into

account regional as well as distant metastases.

Moreover, Hyams (1982) developed a histopathological grading system, based on six parameters related to growth pattern and to other histological findings (lobular architecture, mitotic index, nuclear polymorphism, presence of rosettes, fibrillary matrix, and necrosis). Lesions can be classified in four grades, from 1 to 4, according to the increasing cellular dedifferentiation.

Hyams grading system will be referred to in the next section.

2.4 Pathology Features

Due to the rarity of these tumours, practicing pathologists are not always aware of their distinctive clinical, radiographic, histologic, immunohistochemical, and molecular features. These cases are frequently submitted for consultation, further suggesting the diagnostic difficulties inherent to these tumours (Thompson LD 2009, Schwaab G 1988, Olsen 1983).

Macroscopic

The tumour is usually a unilateral, polypoid, glistening, soft, red grey mass with an intact mucosa . The cut surface appears grey-tan to pink-red and hypervascular (Fig. 3).

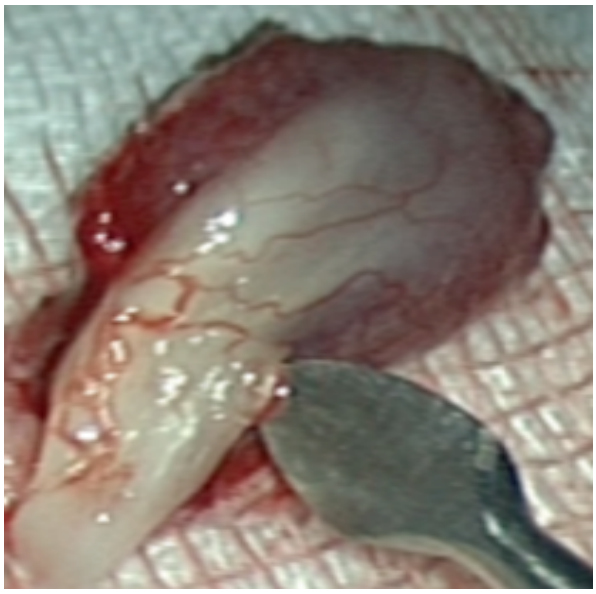

Figure 3: Olfactory bulb with the ONB in the anterior part

Tumours range from <1 cm up to large masses involving the nasal cavity and intracranial region. Tumours frequently expand into the adjacent paranasal sinuses, orbits and cranial vault (Thompson LD 2009).

For practical purposes, the cribriform plate region is involved by the tumour to some degree or another.

Microscopic

The olfactory epithelium contains three cell types, which can be histologically identified in the tumour: basal cells, olfactory neurosensory cells, and supporting sustentacular cells. The basal cells are the stem cell compartment, continuously replacing the neurosensory cells throughout adult life, both physiologically and as a response to injury.

One of the most important histologic features is a lobular architecture comprised of "primitive" neuroblastoma cells. These circumscribed lobules or nests of tumour are identified below an intact mucosa separated by a vascularized fibrous stroma. While in situ tumour is theoretically possible, by the time the tumour reaches clinical attention, in situ disease alone is no longer appreciated. The tumour cells are "small, round, blue" cells slightly larger than mature lymphocytes, with a very high nuclear to cytoplasmic ratio. The nuclei are small and uniform with hyperchromatic, albeit delicate, uniform, "salt-and-pepper" nuclear chromatin distribution. Nucleoli are inconspicuous. The cells are often in a syncytial arrangement with a tangle of neuronal processes forming the background. Cellular nests are surrounded by fine fibrovascular septa in an organoid fashion. The matrix is finely fibrillar. While high grade lesions exist (discussed below), for the most part, nuclear pleomorphism, mitotic figures (>2/HPF), and necrosis are uncommon. Two types of rosettes are recognized: pseudorosettes (Homer Wright) seen in up to 30% of cases, and true rosettes (Flexner-Wintersteiner) seen in about 5% of cases. The delicate, neurofibrillary and edematous stroma forms in the center of a cuffing or palisaded arrangement of cells in Homer Wright pseudorosettes, while a "gland-like" tight annular arrangement is seen in Flexner-Wintersteiner rosettes. The latter is comprised of gland-like spaces lined by non-ciliated columnar cells with basally placed nuclei. Peritheliomatous "rosettes" are of no diagnostic utility. Variable amounts of calcification may be seen, although they are not usually present in higher grade tumours (Grades III and IV). Exceedingly uncommon, vascular invasion, ganglion cells, melanin-containing cells and rhabdomyoblastic cells can be identified.

Tumours are separated into four grades, although sometimes a definitive separation between grades is arbitrary. There is a continuum from Grade I to Grade IV (see Table 3), with grade based on the degree of differentiation, presence of neural stroma, mitotic figures, and necrosis. Lobularity is present in all tumours, although better developed in Grade I tumours, but still present in Grade IV lesions. Grade I includes the majority of tumours and is the most differentiated. The cells are syncytial, have cytoplasmic neurofibrillary extensions, and are uniform, with small round nuclei and evenly disbursed nuclear chromatin. Surrounding fibrous stroma is quite vascular. Mitotic activity and necrosis is absent. Grade II tumours show less neurofibrillary stroma and slightly more pleomorphism, with isolated mitoses. Grade III tumours show more pleomorphism, coarse chromatin distribution, hyperchromasia, with increased mitotic activity and necrosis. Flexner-Wintersteiner rosettes may be seen and calcifications are absent. Grade IV neoplasms are the most anaplastic, showing pleomorphic nuclei with prominent eosinophilic nucleoli. Necrosis increased mitotic figures, including atypical mitotic forms are common. Neurofibrillary material is absent, as are calcifications. The grade correlates with prognosis, although not as sensitively as tumour stage. As the grade of the tumour increases so does the difficulty in diagnosis, often requiring ancillary studies to confirm the diagnosis (Thompson LD 2009).

Table 3: Hyams' grading system

Olfactory neuroblastoma grading (based on Hyams' grading system)

Microscopic features	Grade I	Grade II	Grade III	Grade IV
Architecture	Lobular	Lobular	±Lobular	±Lobular
NF matrix	Prominent	Present	May be present	Present
Rosettes	HR	HR	FW	FW
Mitoses	Absent	Present	Prominent	Marked
Necrosis	Absent	Absent	Present	Prominent
Glands	May be present	May be present	May be present	May be present

Microscopic features	Grade I	Grade II	Grade III	Grade IV
Calcification	Variable	Variable	Absent	Absent

NF neurofibrillary, *HR* Homer Wright pseudorosettes, *FW* Flexner-Wintersteiner rosettes

Histochemical studies

The increased utilization of immunohistochemistry studies has made histochemical reactions less valuable, but occasionally the silver stains such as Bodian, Grimelius and Churukian-Schenk may still be of assistance in highlighting the neurosecretory granules (Thompson LD 2009).

Ultrastructural features

Membrane-bound dense core neurosecretory granules are present in the cytoplasm and in nerve processes, which additionally contain neurotubules and neurofilaments. The diameter of the granules is from 50 to 250 nm. Olfactory differentiation with olfactory vesicles and microvilli or apical cilia on apical borders may be seen in Flexner-Wintersteiner rosettes. The fibrillary stroma corresponds to the immature nerve processes. Schwann-like cells are uncommon (Thompson LD 2009).

Immunohistochemical features

ONBs are positive for synaptophysin, chromogranin, CD56, neuron specific enolase, NFP and S-100 protein. The small round cells are usually positive for the first five markers whereas the S-100 protein-positive cells are found at the periphery of the tumour lobules and correspond to Schwann (sustentacular) cells. These same peripheral cells may be positive with glial filament acidic protein (GFAP). Class III beta-tubulin and EPCAM are positive. A few ONBs may also stain focally for low molecular weight cytokeratin (Cam 5.2). They are negative, however, for desmin, myogenin,

CD45RB (leukocyte common antigen), as well as CD99 (MIC2 antigen). Proliferation marker studies using Ki-67 reveal a high proliferative index of 10–50%. Aneuploidy and polyploidy is frequent, but not germane in diagnosis (Thompson LD 2009, Schmidt JT 1990).

Table 4: Immunohistochemical features of olfactory neuroblastoma

positive	negative
neuron specific enolase (NSE) synaptophysin cromogranine A S-100 neurofilament protein (NFP)	Cytokeratin epithelial membrane antigen (EMA) carcinoembryonic antigen (CEA) CD45 CD99 HMB45 Melan A Desmin

The differential diagnosis of olfactory neuroblastoma includes the group of small round cell malignant neoplasms that can occur in the sinonasal tract, i.e., sinonasal undifferentiated carcinoma, lymphoma, rhabdomyosarcoma, mucosal malignant melanoma and neuroendocrine carcinomas.

Neuroendocrine carcinomas (NEC) include, among different tumour types, the carcinoid tumour, atypical carcinoid tumour and small cell carcinoma. NEC of the sinonasal tract are extraordinarily rare, and in contrast to the larynx, the most common subtype is small cell carcinoma. By light microscopy, small cell carcinoma typically is a submucosal hypercellular proliferation growing in sheets, cords and ribbons; the distinct lobular pattern of olfactory neuroblastoma is absent. The cells are small and hyperchromatic with oval to spindle shaped nuclei, absent nucleoli and mini- mal cytoplasm. Cellular pleomorphism, high nuclear to cytoplasmic ratio, high mitotic activity, confluent necrotic areas and individual cell necrosis are readily apparent as well as lymphovascular and perineural invasion. Characteristically, crush artifacts of the neoplastic cells are seen. Squamous cell foci may occasionally be present; glandular or ductal differentiation is rarely seen. Although uncommon, neural type rosettes similar to those seen in olfactory neuroblastoma can be seen in association with small cell carcinoma. The overall light microscopic findings should allow

for differentiating small cell carcinoma from olfactory neuroblastoma in most cases, but immuno-histochemical evaluation may be required in some cases. The immunohistohemical profile of small cell carcinoma includes variable reactivity for cytokeratin, chromogranin, synaptophysin, neuron specific enolase (NSE), S-100 protein and thyroid transcription factor-1 (TTF-1). Cytokeratin reactivity may include a punctate paranuclear or globoid pattern. The tumour usually is negative for cytokeratin, and the positive cases do not show a punctate paranuclear or globoid pattern. In contrast to olfactory neuroblastoma, NSE reactivity in small cell carcinoma is more likely to be focal than diffusely positive, and the S100 protein staining, if present, is dispersed through out the cellular proliferation and not limited to sustentacular cells. Olfactory neuroblastoma is also negative for TTF-1 (Barnes L 2005).

2.5 Differential Diagnosis

The differential diagnosis of ONB includes the group of “small round blue cell” malignant neoplasms that can occur in the sinonasal tract, i.e. squamous cell carcinoma, sinonasal undifferentiated carcinoma, extranodal NK/T cell lymphoma, nasal type, rhabdomyosarcoma, Ewing/PNET, mucosal malignant melanoma and neuroendocrine carcinomas (NEC). Of course, a metastic adrenal gland neuroblastoma to the sinonasal tract would present with histologically identical findings but a lack of MYCN amplification would help to make this separation. Interestingly, NEC tend to be high grade lesions, with necrosis, high mitotic figures, and apoptosis. These tumours will show a punctate paranuclear cytokeratin immunoreactivity that is not seen in the cases of ONB that react with keratin. ONB is also nonreactive with TTF-1, while NEC can be positive. Other tumours considered in the differential diagnosis are paraganglioma, extramedullary plasmacytoma, pituitary adenoma, extracranial meningioma, mesenchymal chondrosarcoma, and granulocytic sarcoma. In a small biopsy with crush artifact, misinterpretation is common, especially as edge effect and diffuse artifacts with immunohistochemistry may not resolve the differential (Table 5). As an example, keratin reactions can be positive in up to one-third of ONBs and in a well defined subset of alveolar rhabdomyosarcomas, besides being positive in the epithelial neoplasms mentioned above. Therefore, extra caution should be employed when making an interpretation on limited material (Thompson LD 2009).

Table 5: Features for differential diagnosis

Feature	Olfactory neuroblastoma	Sinonasal undifferentiated carcinoma	Ewing sarcoma/PNET	Neuroendocrine carcinoma
Mean age	40–45 years	55–60 years	<30 years	50 years
Site	Roof of nasal cavity	Multiple sites usually	Maxillary sinus > nasal cavity	Superior/posterior nasal cavity, ethmoid, maxillary sinuses
Imaging studies	"Dumbbell-shaped" cribriform plate mass	Marked destruction/spread	Mass lesion with bone erosion	May invade skull base or orbit
Prognosis	60–80% 5-year survival	<20% 5-year survival	60–70% 5-year (stage, size, *FLI1*)	>60% die of disease
Cranial nerve involvement	Sometimes	Common	Sometimes	Uncommon
Pattern	Lobular	Sheets and nests	Sheets, nests	Ribbons, islands
Cytology	Salt and pepper chromatin, small nucleoli (grade dependent)	Medium cells, inconspicuous nucleoli	Medium, round cells, vacuolated cytoplasm, fine chromatin	Salt and pepper, granular chromatin
Anaplasia	Occasionally and focally	Common	Minimal	Moderate
Mitotic figures	Variable	High	Common	High
Necrosis	Occasionally	Prominent	Frequent	Prominent
Vascular invasion	Occasionally	Prominent	Rare	Present
Neurofibrillary stroma	Common	Absent	Absent	Absent
Pseudorosettes	Common	Absent	Present	Present
Keratin	Focal, weak	>90%	Rare	Positive
CK 5/6	Negative	Negative	n/a	n/a

Feature	Olfactory neuroblastoma	Sinonasal undifferentiated carcinoma	Ewing sarcoma/PNET	Neuroendocrine carcinoma
EMA	Negative	50%	n/a	n/a
NSE	>90%	50%	Positive	Positive
S-100 protein	+ (sustentacular)	<15%	Rare	Positive
Synaptophysin	>90% (can be weak)	<15%	Positive	Positive
In situ EBER	Absent	Absent	Absent	Absent
Neurosecretory granules (EM)	Numerous	Rare	Absent	Present

EBER Epstein barr virus encoded RNA (EBV-encoded RNA)

Modified From: Thompson 2009

2.6 Treatment guidelines and outcome

According to the results of a recent meta-analysis (Dulguerov et al. 2001), the combination of surgery and radiotherapy was associated with the highest 5- year survival rate (65%). In particular, the management of olfactory neuroblastoma has been radically changed by the introduction of anterior craniofacial resection, which has the advantage to ensure an adequate margin of excision even at the level of the anterior cranial fossa (Ketcham AS et al 1963). This approach, followed by postoperative radiotherapy, is currently considered the gold standard for lesions without gross brain infiltration. In case of advanced-stage disease or of a poorly differentiated olfactory neuroblastoma, patients should instead undergo chemotherapy, either alone or combined with surgery and/or radiotherapy (Levine et al. 1999). Cisplatin, doxorubicin, etoposide, and vincristine have been used in different combinations (Eich et al. 2001; Simon et al. 2001; Lundet al. 2003). However, platinum-based regimens seem to be associated with the best responses (Sheehan et al. 2000).

In recent years, promising results in the management of selected cases of olfactory neuroblastoma mostly limited to the naso-ethmoidal complex have been reported with the use of a micro-endoscopic approach (Stammberger et al. 1999; Casiano et al. 2001; Cakmak et al. 2002; Folbe et al. 2009). Postoperative stereotactic radiotherapy has been added with the intent to optimize the local control of the disease and, at the same time, to minimize the morbidity (Walch et al. 2000). Additional experience with a long postoperative follow up is certainly warranted to definitively establish the role of such an alternative approach.

The presence of cervical node metastasis requires an adequate neck dissection and/or radiotherapy (according to the treatment selected for the primary lesion). Since an extremely variable rate of cervical metastases is reported in the literature, elective treatment is a matter of debate. As a matter of fact, it seems reasonable to assess the status of retropharyngeal as well as of cervical lymph nodes by imaging studies and to treat the neck only in those patients who have positive nodes.

Local recurrence, which occurs in 17%-30% of patients, is the most frequent cause of treatment failure, whereas regional recurrence and distant metastases may account for up to 20% and 4%,

respectively (Lund et al. 2003). While local and regional recurrences are amenable to salvage treatment in 33-50% and one third of patients, respectively, distant metastases almost invariably carry an ominous prognosis (Dulguerov et al. 2001).

A very peculiar finding to keep in mind with olfactory neuroblastoma is that local recurrences may occur even many years after treatment. In the paper by Lund et al. (1998), 5-year actuarial survival was 62%, but at 10 years survival dropped down to 47%. The high rate of late recurrences explain why in olfactory neuroblastoma patients follow up surveillance must be extended for at least 10 years.

Prognosis of olfactory neuroblastoma is correlated not only to the extension of the lesion, but also to Hyams's histopathologic grade (Miyamoto et al. 2000). Other factors having an impact on survival are the presence of metastatic lymph nodes (Koka et al. 1998) and shrinkage of the lesion after chemotherapy (McElroy et al. 1998; Morita et al. 1993).

There is an associated decrease in survival as the stage increases: 75–91% for Stage A, 68–71% for Stage B and 41–47% for Stage C. Most tumours are in Stage C (about 50%). Overall, there is a 60–80% 5-year survival (stage and grade dependent). Low grade tumours have an 80% 5-year survival while high grade tumours have a 40% survival (Thompson LD 2009).

Table 6: percentage of survival according to stage (Kadish S 1976)

Stage	Extent of tumour	5-Year survival (%)
A	Tumour confined to the nasal cavity	75–91
B	Tumour involves the nasal cavity plus one or more paranasal sinuses	68–71
C	Extension of tumour beyond the sinonasal cavities	41–47

Complete surgical elimination frequently requires a bicranial-facial approach which removes the cribriform plate, and is usually followed by a course of radiotherapy as the treatment of choice to achieve the best long term outcome. Occasionally, endoscopic resection for limited tumour can achieve similar results. An elective neck dissection is not warranted. Palliation with chemotherapy is achieved for advanced unresectable tumours or for disseminated disease (Eriksen JG 2000). Autologous bone marrow transplantation has achieved long term survival in limited cases. The tumours tend to be locally aggressive, involving adjacent structures (orbit and cranial cavity). Depending on stage and grade of tumour, patient survival ranges from 78% at 5 years to 68% at 15 years. As a point of comparison, low grade tumours have a reported 80% 5-year survival compared to 40% 5-year survival for high-grade tumours. Recurrences develop in about 30% of patients (range 15–70%), usually within the first 2 years after initial management. Cervical lymph node metastasis (up to 25%) or distant metastases (approximately 10%) develop irrespective of the grade of the tumour. The most frequent sites of distant metastasis are the lungs and bones. Overall survival is adversely affected by female gender, age <20 or >50 years at initial presentation, high tumour grade, extensive intracranial spread, distant metastases, tumour recurrence, a high proliferation index, and polyploidy/aneuploidy (Thompson LD 2009).

3. ARRAY COMPARATIVE GENOMIC HYBRIDIZATION

3.1 a-CGH definition and technique

Cytogenetics is a branch of genetics that is concerned with the study of the structure and function of the cell, especially the chromosomes. It includes routine analysis of G-Banded chromosomes, other cytogenetic banding techniques, as well as molecular cytogenetics such as fluorescent in situ hybridization (FISH) and comparative genomic hybridization (CGH).

Comparative genomic hybridization (CGH) is a molecular-cytogenetic method for the analysis of copy number changes (gains/losses) in the DNA content of a given subject's DNA or in the DNA of tumour cells.

Array comparative genomic hybridization (a-CGH) is a modern technique to detect genomic copy number variations at a higher resolution level than chromosome-based comparative genomic hybridization (CGH).

First published in 1992, CGH is the first genome-wide method in detecting DNA copy numbers alterations. In the original method, total genomic DNA is isolated from test and reference samples, differentially labeled and hybridized to metaphase chromosomes from normal individuals (Kallioniemi et al. 1992). Measuring the fluorescence intensity ratio along each chromosome reveals the gain or loss in the test sample relative to reference sample at a genome wide scale.

Microarray with smaller elements can potentially provide higher genomic resolution (Carter 2007).

Recently, CGH technique uses commercial oligonucleotide array platform with high resolution, ready for use availability, and relatively low price (Ylstra 2006).

3.2 a-CGH and olfactory neuroblastoma

The cytogenic data for ONB are limited. Early suggestions that ONB is a form of peripheral neuroectodermal tumour 52 have been subsequently disproven in multiple studies. In these studies, reverse transcriptase-PCR or FISH failed to find the EWS-FLI1 fusion transcript or EWS rearrangement in any candidate ONB. These findings explain the demonstrated absence of CD99 immunohistochemical staining in ONB.25

In 1997 Szymas et al describe genomic imbalances of olfactory neuroblastoma in a 46-year-old woman by using the molecular cytogenetic technique - comparative genomic hybridization (CGH) for the first time in order to define the spectrum of genetic abnormalities in the tumour.

The CGH analysis showed multiple changes including DNA overrepresentations of chromosomes 4, 8, 11 and 14, partial DNA gains of the long arms of chromosomes 1 and 17, deletions of the entire chromosomes 16, 18, 19 and X, and partial losses of chromosomes 5q and 17p. This study represents an early utilisation of the CGH technique in olfactory neuroblastoma and demonstrates that the tumour carries complex chromosomal aberrations (Szymas 1997).

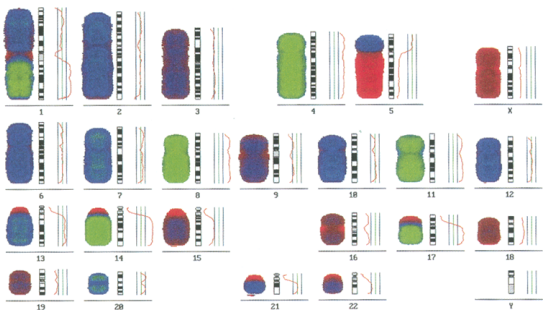

Figure 4: CGH analysis showed in Szymas' paper

Fig: CGH analysis of the tumour. Nine metaphases were evaluated and summerized in aCGH-sum-karyogram.Deletions are depicted in red color, amplifications in green and equilibrium between tumour and normal DNA in blue. DNA gains of entire chromosomeswere observed for chromosomes4, 8, 11 and 14. Partial gains were seen for the long arms of chromosomes 1 and 17. Chromosomes 16, 18, 19 andXwere entirely lost. Partial deletions occurred for chromosomes 5q

and 17p. Since the profiles of chromosomes 3, 9 and 15 were on the threshold line for a deletion they cannot be un ambigiously interpreted as a DNA loss.

In the study of Riazimand the genomic imbalances of three ONB were analyzed by CGH to evaluate a recurrent pattern of imbalances and its relation to the pPNET family. The CGH analysis revealed multiple recurrent aberrations including DNA overrepresentations of chromosomal material of the entire chromosome 19, partial gains of the long arms of chromosomes 8, 15, and 22, and deletions of the entire long arm of chromosome 4. Beside these common aberrations, several single gains and losses occurred, that is, gains on 6p, 10q, 1p, 9q, and 13q. Their findings confirmed the former observation of amplified genetic material on chromosome 8 and found several new, currently not described recurrent genetic aberrations distinct from those described for pPNET and give evidence that ONB is not part of the pPNET family. They suggest that the combined gain of genetic material on 15q, 22q, and chromosome 8 might be indicative for ONB (Riazimand 2002).

Bockmuhl et al. reported on findings in ONB by conventional comparative genomic hybridization including frequent deletions of 1p, 3p/q, 9p, and 10p/q, and amplifications of 17q, 17p13, 20p, and 22q. They also noted a deletion on chromosome 11 and gain on chromosome 1p, which were apparently associated with metastasis and a worse prognosis. The study included 12 patients.

Table 7: Most common alterations in ONB found in Bockmuhl's paper

	DNA losses	DNA gains
Frequency of alterations		
90-100%	3p12-p14	17q12, 17q25
>80%	1p21-31, 3p/q, 9p, 10p/q	17p13, 20q, 22q11.2, 22q13
>70%	12q21,	7q11.2, 11q13, 14q32.2, 16p11.2, 16p13.3, 17q21-q24, 20p
>50%	1q24-q32, 2q22-q32, 4p/q, 5p14, 5q, 6q14-q23, 9q22-q33, 12p11.2-p12, 13q, 18q, 21q21	1q12, 14q, 16q, 19p/q
Pronounced deletions	4p13-p15, 10q26, 13q21-q23	
Pronounced gains		1p34, 1q23-q31, 7p21, 7q31, 9p23-p24, 17q11-q22, 17q24-q25, 19, 20p, 20q13, 22q13
Alterations associated with		
worse prognosis	4p/q, 5p/q, 6q, 7q31-q32, 9p, 11p/q,15q21	1q12, 8q, 20q
metastasis formation	5p/q, 6q, 7q31-q32, 11p12-p14, 11q14-q22, 15q21	1p32-p34, 1q12, 2p22-p24

Another study by Holland et al. has similarly shown complex cytogenetic changes in ONB. They performed comprehensive cytogenetic analyses of an ONB, Hyam's grade III-IV, using trypsin-Giemsa staining (GTG banding), multicolor fluorescence in situ hybridization (M-FISH), and locus-specific FISH complemented by molecular karyotyping using high-density single nucleotide polymorphism arrays. Therefore, their study supported the usefulness of applying complementary methods for cytogenetic analysis (Holland 2007) (Fig. 5).

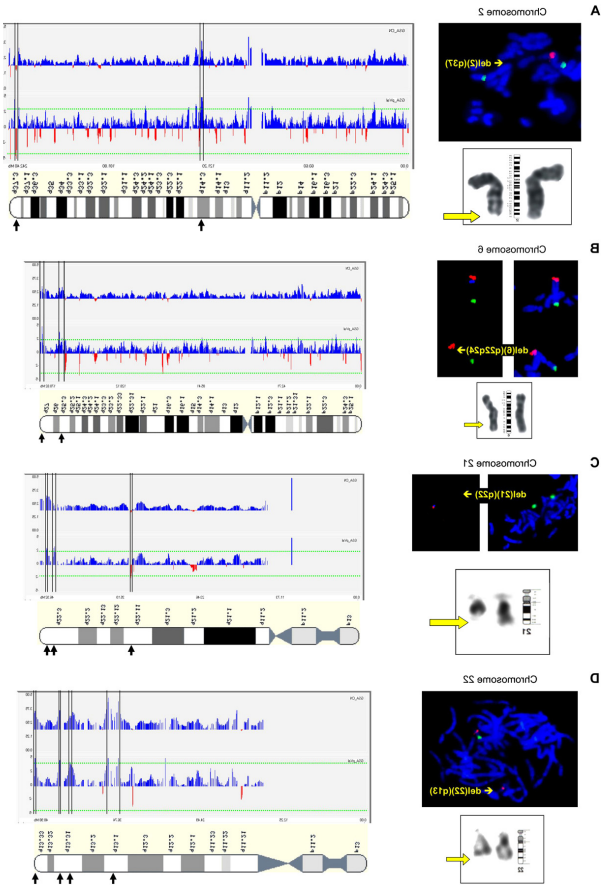

Figure 5: cytogenetic features showed in Holland's paper

Guled et al. performed an oligonucleotide-based aCGH analysis on 13 olfactory neuroblastoma samples, which was the first time that array-based CGH was applied to study the copy number changes in this neoplasm. Several copy number changes reported in previous studies were observed

in their study, with identical, overlapping, or slightly different minimal common regions of alteration. Gains at the distal parts of 1p, 4, 9p, 13q, 15q, 22q, and 21q, and deletions at 4p and X, were reported in at least one study. Gains at 7q11 and 20q and deletions at 2q, 5q, 6p, 6q, and 18q were detected in two studies.

Overall, olfactory neuroblastomas have highly complex copy number changes that occur over the entire genome. All samples analyzed showed genomic imbalances with slightly more gains than losses. a-CGH revealed more copy number changes than previous studies that used conventional CGH. Furthermore, their results showed novel aberrations, which were not described in previous reports. In accordance with at least two previous studies, they found gains at 7q11.2 and 20q13, and losses at 2q31–q37, 5q, 6p, 6q, and 18q. In addition to these previously reported alterations, they identified novel gains in their samples at 5q34–q35, 6p12.3, 10p12.31, 12q23.1–q24.31, and all of chromosome X. Losses at 15q11.2–q24.1, 15q13.1, 19q12–q13, 22q11.1–q11.21, 22q11.23, and 22q12.1 have not been described previously.

They identified a 770 kb region of chromosomal gain at 7q11.2. This region has been implicated in other cancers, and is overexpressed in prostate carcinomas, adenoid cystic carcinomas, head and neck squamous cell carcinomas, and pancreatic endocrine tumours.

A 6 Mb region of gain at 20q13.32–q13.33 was also identified. DNA copy number increases at chromosome 20q13 have been observed frequently in a variety of cancers, including breast, ovarian, and squamous cell carcinomas, suggesting that the region harbors one or more oncogenes.

Losses occurring at chromosome 2q have been described for various carcinomas, including head and neck squamous cell carcinoma, breast carcinoma, lung carcinoma, neuroblastoma, cervical cancer and prostate adenocarcinoma. Studies using different approaches have increasingly shown that the most affected region is 2q32–q37. This region also seems to be implicated in the development of ONB, as it has been reported in three cytogenetic studies including their investigation.

Another area of loss identified in their study, and also reported by Bockmuhl et al. and Holland et al., is located at 6q21–22. This region is frequently deleted in a variety of neoplasms, including pancreatic endocrine tumours, prostate carcinoma, breast carcinoma, and central nervous system lymphomas.

Their study also identified two small gains at 9p13.3 (782 kb) and 13q34 (363 kb) that were previously reported by Holland et al. The 9p13.3 locus has been shown to be gained in prostate cancer cell lines in two recent studies using aCGH. Gains at 13q34 have also been described previously in different cancers, including breast cancer, hepatocellular carcinoma, esophageal squamous cell carcinoma, and lung adenocarcinoma.

As for most tumours, stage is the most important parameter associated with survival in olfactory neuroblastoma. Their results clearly indicate that alterations in 20q and 13q are important in the progression of olfactory neuroblastoma. Gain of 20q has been widely associated with progression of several tumours, including breast carcinoma, cervical carcinoma, and pancreatic carcinoma. Both losses and gains of chromosome 13q have been noted in many recent studies of various tumours, suggesting the existence of novel oncogenes or tumour suppressor genes or both in this region. Furthermore, this region has been reported to contain microRNAs that could function as tumour suppressor genes or oncogenes.

Gains of both 13q and 20q are seen in colorectal carcinomas and their progression.

A number of genes located at these sites have been suggested to be important, but none of these changes has been sufficiently recurrent overall to be helpful in diagnosis, prognosis, or treatment and there have been no single gene mutations found in ONB to unify the entity or aid in its diagnosis. These various studies have, however, identified candidate regions for further study (Faragalla Adv Anat Pathol 2009).

4. MATHERIALS AND METHODS

4.1 Patients

From 1999 to 2011, 24 patients with histologically confirmed ONB were treated at Policlinico S. Matteo, University of Pavia, Ospedale di Circolo, University of Insubria, and Ospedali Civili di Brescia, University of Brescia.

The Kadish system was used to stage the tumour, and Hyams' grading was used to histologically differentiate the tumours. In every case the diagnosis of ONB was established on H&E stained tissue sections and based on the microscopic findings.

All patients underwent our preoperative protocol (Table 8).

Table 8: preoperative protocol

Preoperative protocol
Contrast-enhanced CT
MRI plus gadolinium
Endoscopic biopsies
Chest radiograph
Neck ultrasonography
Ophthalmological evaluation (when necessary)

All patients were informed about the method of treatment and gave their consent to the therapy. Follow-up of the patients ranged from 1 to 153 months, with a mean of 60 months.

4.2 Surgical technique

All the surgical procedures were performed by senior surgeons. In Kadish A tumours, where a dura resection is not foreseen, sodium fluorescein is administered intratecally before surgery to increase intraoperative identification of cerebrospinal fluid (CSF) leak. Initially, the lesion is divided into sections suitable for histological assessment. In the major lesions, we first perform a cavitation with a microdebrider to reduce the volume of the neoplasm while respecting the boundaries of the mass. Then the base of implant of the tumour is removed using a subperiosteal dissection plane, with the centripetal technique. In this manner, we obtain a clean surgical field with an excellent visualization of all the margins. The skull base is then drilled, usually with a diamond burr, and last, after resection of the ethmoidal roof and the fovea ethmoidalis, we remove the dura mater of the olfactory cleft and the olfactory bulb. During the procedure, we normally map the surgical field with many samplings to minimize the risk of recurrence. This mapping is extremely valuable because, in cases of massive dura involvement or frontal sinus involvement, the endoscopic surgical procedure is converted into an open external approach with bifrontal craniotomy. The same surgical approach described earlier is used in all the patients, but obviously, surgical resection is tailored to the patient's local conditions. In fact, a lesser resection is performed for a Kadish A neoplasm than would be done for Kadish C lesion, which necessitates a greater resection; in this sense, when the nasal septum is in contact only with the tumour, we perform a wide subperiosteal dissection and an extensive drilling of the bone plate. When the septum is infiltrated by the ON, it is resected. As for the whole procedure, the dura resection is also tailored to the neoplasm extension and is guided by frozen sections. In all the patients, it was possible to anatomically spare the contralateral olfactory cleft (Castelnuovo P. et al. 2007, Locatelli D et al 2000).

The key points of our surgical procedure are:

dissection of the lesion,

centripetal technique,

removal of dura mater and olfactory bulb, freezing sections, and

multilayer duraplasty (Fig. 6,7,8) (Nicolai P 2008).

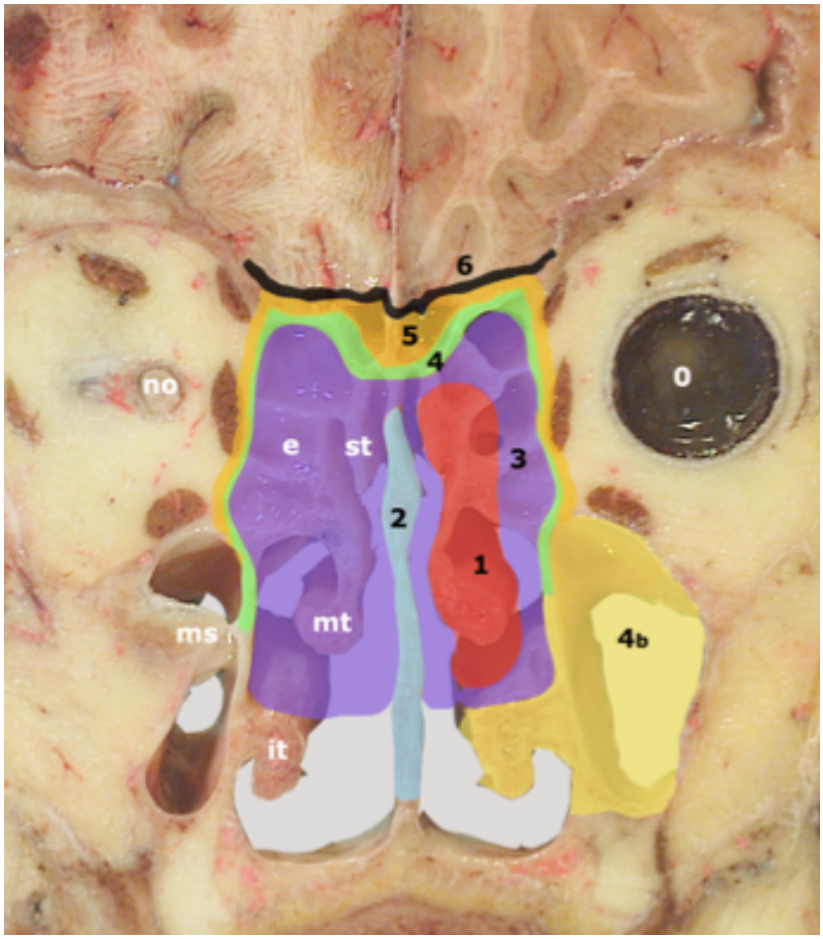

Figure 6: surgical steps in removal ONB

1 red: debulking of the tumour

2 blue: removal of the septum

3 violet: subperiosteal removal of the tumour and Draf III

4 green: removal of the bone/ cartilage in contact with tumour (skull base, lamina papiracea)

5 yellow: removal of the dura mater, olfactory bulb, periorbit, intracranial lesion

6 black: skull base reconstruction with fascia

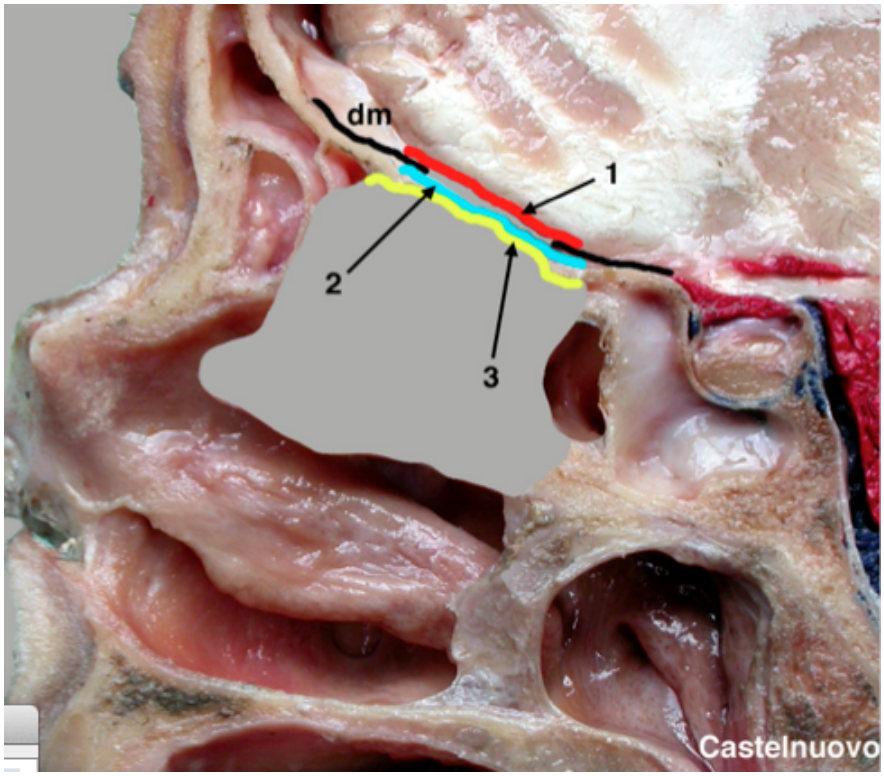

Figure 7: multilayer duraplasty. **Combined closure technique: three grafts: one was inserted deep to the dura, the second was inserted between bone and dura and the third extracranial with the overlay technique.**

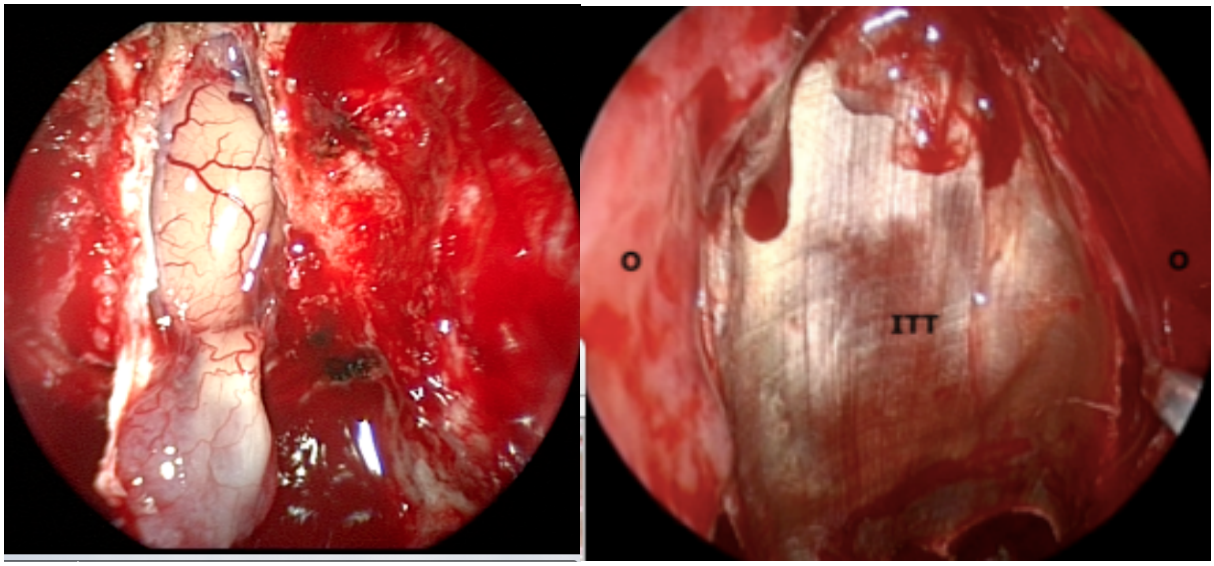

a **b**

Figure 8: endoscopic surgical images of duraplasty. a. large defect of the skull base to repair, b.

fascia placed intracranially

4.3 Radiotherapeutic Technique

Patients underwent postoperative radiotherapy starting 6 to 8 weeks following surgery. A volume encompassing the preoperative extent of the tumour, plus a 5-mm margin, was irradiated at a total dosage of 54 to 60 Gy in 2 Gy daily fractions. All patients were treated by 3-dimensional conformal radiotherapy, including 2 to 3 nonaxial 6 MV photon beams in most cases in order to spare the ocular structures and chiasm, as well as the brain and hypophysis. A narrow spaced (3 mm) CT scan was acquired for target contouring and planning of treatment, the patient's head being immobilized by means of a thermoplastic facemask. Field conformation was achieved by means of customized blocks or multileaf collimators.

4.4 Hystological method

All tissues were fixed in buffered formalin (formaldehyde 4% w/v and acetate buffer 0.05M) and routinely processed to paraffin wax. Five µm-thick sections were stained with hematoxylin-eosin (H&E) for morphological evaluation. For immunohistochemistry, three µm-thick sections were mounted on poly-L-lysine coated slides, deparaffinized and hydrated through graded alcohols to water. After endogenous peroxidase activity inhibition, performed by dipping sections in 3% hydrogen peroxide for 10 minutes, sections were treated in citrate buffer pH 6 in a microwave oven at 750W for 10 minutes for antigen retrieval. Successively, sections were incubated with primary antibodies at 4°C for 18–20 hours, followed by the avidin-biotin complex (ABC) procedure. Immunoreactions were developed using 0.03% 3,3'diaminobenzidine tetrahydrochloride and then sections were counterstained with Harris' hematoxylin. Specificity controls consisted of substitution of the primary antibody with non immune serum of the same species at the same dilution and use of control tissues with or without the pertinent antigen.

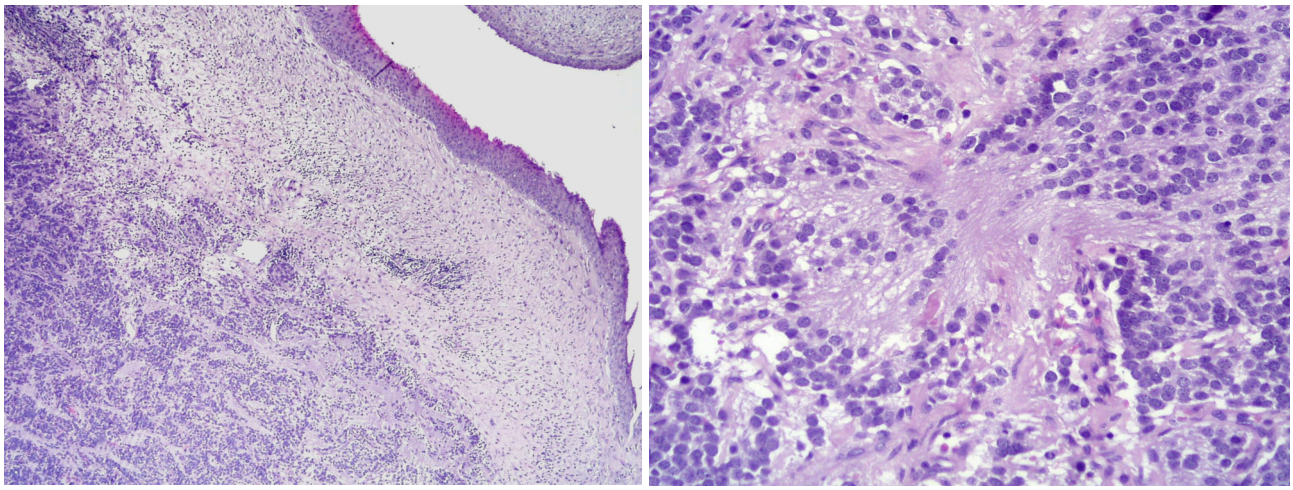

Figure 9: histologic features of ONB

4.5 Technique of a-CGH

At the Biology and Medical Genetics Department of Clinical and Experimental was performed genetic analysis of tumoural DNA using molecular biology techniques-CGH.

The material used for all patients was DNA extracted from material fixed and paraffin-embedded (FFPE) FFPE slices were chosen from anatomy pathologist to contain the majority of cancer cells. Only in 2 patients it was possible to perform the analysis of fresh material.

See the Agilent Oligonucleotide Array-Based CGH for Genomic DNA Analysis (for FFPE Samples) user guide (Version 1.0, P/N G4410-90020) available at www.agilent.com/chem/dnamanuals- protocols for a detailed description of the protocol used.

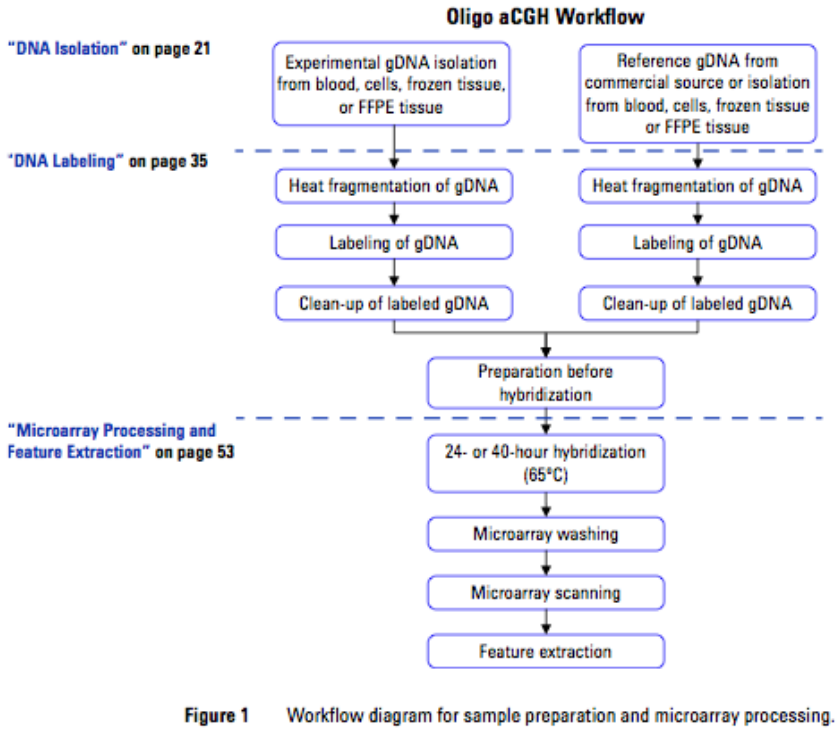

Figure 1 Workflow diagram for sample preparation and microarray processing.

Figure 10: a-CGH workflow diagram for sample preparation and microarray processing

Purification of genomic DNA from formalin-fixed, paraffin-embedded tissues (FFPE)

The procedure to isolate genomic DNA (gDNA) from formalin-fixed paraffin-embedded (FFPE) samples is based on the method described by van Beers et al. (van Beers et al 2006) using the Qiagen DNeasy Blood & Tissue Kit (p/n 69504).

The protocol used is from QIAGEN Technical Service Departments (www.qiagen.com)

Procedure:

Step 1. Paraffin Removal

1 Equilibrate a heat block or water bath to 90 °C and a thermomixer to 37 °C.

2 Put up to 5 20-micron FFPE sections into a 1.5 mL nuclease-free microfuge tube.

3 Prepare 10% Tween 20, by adding 100 µL Tween 20 to 900 µL of nuclease-free water. The solution can be prepared in advance and stored up to 6 months at room temperature.

4 Add 480 µL PBS and 20 µL 10% Tween 20 to the FFPE sections in the 1.5 mL nuclease-free microfuge tube.

5 Transfer the sample tube to a circulating water bath or heat block at 90 °C. Incubate at 90 °C for 10 minutes.

6 Spin immediately for 15 minutes at 10,000 x g in a microcentrifuge. Put the sample tube on ice for 2 minutes.

7 Remove the resulting wax disc with a pipette tip or tweezers. Remove and discard the supernatant without disturbing the pellet.

8 Add 1 mL of 100% ethanol to the pellet and vortex briefly. Spin for 5 minutes at 10,000 x g in a microcentrifuge.

9 Remove ethanol without disturbing the pellet and let the sample tube sit at room temperature with the lid open until residual ethanol has completely evaporated.

10 Prepare a 1M NaSCN solution by adding 10 g of NaSCN to 123 mL of nuclease free water. The solution can be prepared in advance and stored up to 1 month at room temperature.

11 Add 400 µL 1M NaSCN to the dry pellet and briefly mix on a vortex mixer.

12 Transfer the sample tube to a thermomixer at 37 °C. Incubate overnight at 37 °C. Shake at 450 rpm.

Step 2. Proteinase K Treatment

1 Equilibrate a thermomixer to 55 °C.

2 Transfer the sample tube to a microcentrifuge. Spin for 20 minutes at 10,000 x g.

3 Remove and discard the supernatant without disturbing the pellet.

4 Add 400 µL PBS to the pellet and vortex briefly.

5 Spin again for 20 minutes at 10,000 x g in a microcentrifuge.

6 Remove and discard the supernatant without disturbing the pellet.

7 Add 360 µL of Qiagen buffer ATL (supplied with Qiagen DNeasy Blood & Tissue Kit).

8 Add 40 µL proteinase K (supplied), mix well on a vortex mixer, and incubate overnight in a thermomixer at 55 °C shaking at 450 rpm.

9 Transfer the sample tube to a microcentrifuge. Spin for 30 seconds at 6,000 x g to drive the contents off the walls and lid.

10 Add 40 µL proteinase K, mix well on a vortex mixer, and incubate in a thermomixer for approximately 6 to 8 hours at 55 °C shaking at 450 rpm.

11 At the end of the day, transfer the sample tube to a microcentrifuge and spin for 30 seconds at 6,000 x g to drive the contents off the walls and lid.

12 Add 40 µL proteinase K, mix well on a vortex mixer and incubate overnight in a thermomixer at 55 °C shaking at 450 rpm.

Step 3. gDNA Extraction

1 Equilibrate a heat block or water bath to 56 °C.

2 Let samples cool to room temperature and spin in a microcentrifuge for 30 seconds at 6,000 x g to drive the contents off the walls and lid.

3 Add 8 µL of RNase A (100 mg/mL), mix on a vortex mixer, and incubate for 2 minutes at room temperature. Transfer the sample tube to a microcentrifuge and spin for 30 seconds at 6,000 x g to

drive the contents off the walls and lid.

4 Add 400 µL Buffer AL (supplied), mix thoroughly on a vortex mixer, and incubate in a circulating water bath or heat block at 56 °C for 10 minutes. Transfer the sample tube to a microcentrifuge and spin for 30 seconds at 6,000 x g to drive the contents off the walls and lid.

5 Add 440 µL 100% ethanol, and mix thoroughly on a vortex mixer. Transfer the sample tube to a microcentrifuge and spin for 30 seconds at 6,000 x g to drive the contents off the walls and lid.

6 Put two DNeasy Mini spin columns in two clean 2 mL collection tubes (supplied). Split the entire sample mixture onto two DNeasy Mini spin columns (i.e. 660 µL each).

7 Spin in a microcentrifuge for 1 minute at 6,000 x g. Discard the flow-through and collection tube. Put the DNeasy Mini spin columns in fresh 2 mL collection tubes (supplied).

8 Before using for the first time, prepare Buffer AW1 by adding 100% ethanol to the Buffer AW1 bottle (supplied; see bottle label for volume). Mark the appropriate check box to indicate that ethanol was added to the bottle.

9 Add 500 µL Buffer AW1 onto each spin column, and spin in a centrifuge for 1 minute at 6,000 x g. Discard the flow-through and collection tube. Put the DNeasy Mini spin columns in fresh 2 mL collection tubes (supplied).

10 Prepare a fresh 80% ethanol solution by adding 40 mL 100% ethanol to 10 mL nuclease-free water.

11 Add 500 µL 80% ethanol onto each column, and spin in a microcentrifuge for 3 minutes at 20,000 x g to dry the column membrane. Discard the flow-through and collection tube.

12 Put the DNeasy Mini spin column in a clean 1.5 mL microcentrifuge tube, and add 50 µL of nuclease free water directly to the center of each spin column.

13 Let stand at room temperature for 1 minute, and then spin in a microcentrifuge for 1 minute at 6,000 x g to elute the DNA.

14 Combine the purified DNA from the same sample in one microcentrifuge tube for a final total volume of 100 µL.

DNA Labeling

Step 1. Preparation of gDNA Before Labeling

1 Estimate the average molecular weight for each gDNA sample based on the agarose gel analysis

2 If the gDNA concentration isless than required, concentrate the sample using a concentrator before you continue to the heat fragmentation.

3 Put the appropriate amount of gDNA and nuclease-free water in a 0.2 mL nuclease-free PCR tube or plate to achieve the volumes

Step 2. Heat Fragmentation

1 Incubate the gDNA at 95 °C in a thermocycler with heated lid for the time to fragment the gDNA.

2 Transfer the sample tubes to ice and incubate on ice for 3 minutes. You can also hold at 4 °C for 3 minutes in a thermocycler.

3 Spin in a microcentrifuge for 30 seconds at 6,000 × g to drive the contents off the walls and lid.

Step 3. ULS Labeling

1 Prepare one Cy3 and one Cy5 Labeling Master Mix by mixing the components, based on your microarray format and sample type. Avoid pipetting volumes less than 2 µL to ensure accuracy.

2 Add the appropriate amount of Labeling Master Mix to each PCR tube containing the gDNA to make a total volume. Mix well by gently pipetting up and down.

3 Transfer PCR tubes or plates to a thermocycler with heated lid and incubate at 85 °C for 30 minutes.

4 Transfer the samples to ice and incubate on ice for 3 minutes. You can also hold at 4 °C for 3 minutes in a thermocycler.

5 Spin in a microcentrifuge for 1 minute at 6,000 × g to drive the contents off the walls and lid.

Labeled gDNA can be stored on ice until dye removal using the Agilent KREApure columns or the Agilent Genomic DNA 96-well Purification Module.

Step 4. Removal of non-reacted ULS-Cy

Non-reacted ULS-Cy3 or ULS-Cy5 can interfere with the subsequent microarray experiment and increase background noise if they are not efficiently removed prior to hybridization. The Agilent KREApure columns or Genomic DNA 96-well Purification Module effectively removes non-reacted ULS dye.

Preparation of Labeled Genomic DNA for Hybridization

1 Prepare the 100X Blocking Agent:

a Add 135 µL of nuclease-free water to the vial containing lyophilized 10X CGH Blocking Agent (supplied with Agilent Oligo aCGH Hybridization Kit).

b Mix briefly on a vortex mixer and leave at room temperature for 60 minutes to reconstitute sample before use or storage.

c Cross out “10X” on the label on the blocking agent vial and write “100X”. You are actually making a 100X Blocking Agent, so you need to relabel the

vial of lyophilized blocking agent as such.

The 100X Blocking Agent can be prepared in advance and stored at -20 °C.

2 Equilibrate water baths or heat blocks to 95 °C and 37 °C or use a thermocycler.

3 Prepare the Hybridization Master Mix by mixing the components in the table below according to the microarray format.

4 Add the appropriate volume of the Hybridization Master Mix to the 1.5 mL microfuge tube, tall chimney plate well or PCR plate well containing the labeled gDNA to make the total volume

5 Mix the sample by pipetting up and down, and then quickly spin in a centrifuge to drive the contents off the walls and lid.

6 Incubate the samples:

a Transfer sample tubes to a circulating water bath or heat block at 95 °C.

Incubate at 95 °C for 3 minutes.

b Immediately transfer sample tubes to a circulating water bath or heat block at 37 °C. Incubate at 37 °C for 30 minutes or Transfer sample tubes to a thermocycler. Program the thermocycler

7 Remove sample tubes from the water bath, heat block or thermocycler. Quickly spin in a centrifuge to drive the contents off the walls and lid.

8 Bring the Agilent-CGHblock (supplied with the ULS Labeling Kit) to room temperature.

Make sure that the Agilent-CGHblock is completely equilibrated to room temperature before you continue.

9 Add the appropriate volume of Agilent-CGHBlock to each well or 1.5 mL microfuge tube containing the labeled gDNA and Hybridization Master Mix to make the final volume of hybridization sample mixture.

Mix well by pipetting up and down.

10 Quickly spin in a centrifuge to drive the contents off the walls and lid.

Microarray Processing and Feature Extraction

Step 1. Microarray Hybridization

Step 2. Wash Preparation

Step 3. Microarray Washing

Step 4. Microarray Scanning using Agilent SureScan, C or B Scanner

Step 5. Data Extraction using Feature Extraction Software

Microarray processing consists of hybridization, washing, and scanning.

Feature Extraction is the process by which data is extracted from the scanned microarray and translated into log ratios, allowing researchers to measure DNA copy number changes in their experiments in conjunction with Agilent Genomic Workbench Software.

Step 1. Microarray Hybridization

Hybridization Assembly

1 Load a clean gasket slide into the Agilent SureHyb chamber base with the gasket label facing up and aligned with the rectangular section of the chamber base. Ensure that the gasket slide is flush with the chamber base and is not ajar.

2 Slowly dispense 490 µL (for 1x microarray), 245 µL (for 2x microarray), 100 µL (for 4x microarray) or 40 µL (for 8x microarray) of hybridization sample mixture onto the gasket well in a "drag and dispense" manner. For multi-pack microarray formats (i.e. 2x, 4x or 8x microarray), load all gasket wells before you load the microarray slide. For multi-pack formats, refer to "Agilent Microarray Layout and Orientation"

3 Put a microarray slide "active side" down onto the gasket slide, so the numeric barcode side is facing up and the "Agilent"-labeled barcode is facing down. Assess that the sandwich-pair is properly aligned.

4 Put the SureHyb chamber cover onto the sandwiched slides and slide the clamp assembly onto both pieces.

5 Hand-tighten the clamp firmly onto the chamber.

6 Vertically rotate the assembled chamber to wet the slides and assess the mobility of the bubbles. Tap the assembly on a hard surface if necessary to move stationary bubbles.

7 Put assembled slide chamber in the rotator rack in a hybridization oven set to 65 °C. Set your hybridization rotator to rotate at 20 rpm.

8 Hybridize at 65 °C: • 24 hours for blood, cell and tissue samples (4x and 8x microarrays) • 40 hours for blood, cell and tissue samples (1x and 2x microarrays) • 40 hours for FFPE samples (1x,

2x, 4x and 8x microarray)

Step 2. Wash Preparation

Cleaning with Milli-Q Water Wash

Rinse slide-staining dishes, slide racks and stir bars thoroughly with high-quality Milli-Q water before use and in between washing groups.

a Run copious amounts of Milli-Q water through the slide-staining dishes, slide racks and stir bars.

b Empty out the water collected in the dishes at least five times. c Repeat step a and step b until all traces of contaminating material are removed.

Cleaning with Acetonitrile Wash

Acetonitrile wash removes any remaining residue of Agilent Stabilization and Drying Solution from slide-staining dishes.

a Add the slide rack and stir bar to the slide-staining dish, and transfer to a magnetic stir plate.

b Fill the slide-staining dish with 100% acetonitrile.

c Turn on the magnetic stir plate and adjust the speed

d Wash for 5 minutes at room temperature.

e Discard the acetonitrile as is appropriate for your site.

f Repeat step a through step e.

g Air dry everything in the vented fume hood.

h Continue with the Milli-Q water wash as previously instructed.

Prewarming Oligo aCGH Wash Buffer 2 (Overnight)

The temperature of Oligo aCGH Wash Buffer 2 must be at 37 °C for optimal performance.

1 Add the volume of buffer required to a disposable plastic bottle and warm overnight in an incubator or circulating water bath set to 37 °C.

2 Put a slide-staining dish into a 1.5 L glass dish three-fourths filled with milli-Q water and warm

to 37 °C by storing overnight in an incubator set to 37 °C.

Prewarming Stabilization and Drying Solution (Wash Procedure B Only)

The Agilent Stabilization and Drying Solution contains an ozone scavenging compound dissolved in acetonitrile. The compound in solution is present in saturating amounts and may precipitate from the solution under normal storage conditions. If the solution shows visible precipitation, warming of the solution will be necessary to redissolve the compound. Washing slides using Stabilization and Drying Solution showing visible precipitation will have profound adverse affects on array performance.

1 Put a clean magnetic stir bar into the Stabilization and Drying Solution bottle and recap.

2 Partially fill a plastic bucket with hot water at approximately 40 °C to 45 °C (for example from a hot water tap).

3 Put the Stabilization and Drying Solution bottle into the hot water in the plastic bucket.

4 Put the plastic bucket on a magnetic stirrer (not a hot-plate) and stir.

5 The hot water cools to room temperature. If the precipitate has not all dissolved replenish the cold water with hot water.

6 Repeat step 5 until the solution is clear.

7 After the precipitate is completely dissolved, allow the solution to equilibrate to room temperature prior to use.

Step 3. Microarray Washing

Wash Procedure A (without Stabilization and Drying Solution)

1 Completely fill slide-staining dish #1 with Oligo aCGH Wash Buffer 1 at room temperature.

2 Put a slide rack into slide-staining dish #2. Add a magnetic stir bar. Fill slide-staining dish #2 with enough Oligo aCGH Wash Buffer 1 at room temperature to cover the slide rack. Put this dish on a magnetic stir plate.

3 Put the prewarmed 1.5 L glass dish filled with water and containing slide-staining dish #3 on a magnetic stir plate with heating element. Fill the slide-staining dish #3 approximately three-fourths

full with Oligo aCGH Wash Buffer 2 (warmed to 37 °C). Add a magnetic stir bar. Turn on the heating element and maintain temperature of Oligo aCGH Wash Buffer 2 at 37 °C; monitor using a thermometer.

4 Remove one hybridization chamber from incubator and resume rotation of the others. Record whether bubbles formed during hybridization and if all bubbles are rotating freely.

5 Prepare the hybridization chamber disassembly. a Put the hybridization chamber assembly on a flat surface and loosen the

thumbscrew, turning counter-clockwise.

b Slide off the clamp assembly and remove the chamber cover.

c With gloved fingers, remove the array-gasket sandwich from the chamber base by lifting one end and then grasping in the middle of the long sides. Keep the microarray slide numeric barcode facing up as you quickly transfer the sandwich to slide-staining dish #1.

d Without letting go of the slides, submerge the array-gasket sandwich into slide-staining dish #1 containing Oligo aCGH Wash Buffer 1.

6 With the sandwich completely submerged in Oligo aCGH Wash Buffer 1, pry the sandwich open from the barcode end only. Do this by slipping one of the blunt ends of the forceps between the slides and then gently twist the forceps to separate the slides. Let the gasket slide drop to the bottom of the staining dish. Remove the microarray slide, grasp it from the upper corners with thumb and forefinger, and quickly put into slide rack in the slide-staining dish #2 containing Oligo aCGH Wash Buffer 1 at room temperature. Minimize exposure of the slide to air. Touch only the barcode portion of the microarray slide or its edges!

7 Repeat step 4 through step 6 for up to four additional slides in the group. A maximum of five disassembly procedures yielding five microarray slides is advised at one time in order to facilitate uniform washing.

8 When all slides in the group are put into the slide rack in slide-staining dish #2, stir using setting 4 for 5 minutes. Adjust the setting to get good but not vigorous mixing.

9 Transfer slide rack to slide-staining dish #3 containing Oligo aCGH Wash Buffer 2 at 37 °C, and stir using setting 4 for 1 minute.

10 Slowly remove the slide rack trying to minimize droplets on the slides. It should take 5 to 10 seconds to remove the slide rack.

11 Discard used Oligo aCGH Wash Buffer 1 and Oligo aCGH Wash Buffer 2.

12 Repeat step 1 through step 11 for the next group of five slides using fresh Oligo aCGH Wash Buffer 1 and Oligo aCGH Wash Buffer 2 pre-warmed to 37 °C.

13 Put the slides in a slide holder.

Figure 11: **Slide in slide holder for SureScan microarray scanner**

Wash Procedure B (with Stabilization and Drying Solution)

Cy5 is susceptible to degradation by ozone. Use this wash procedure if the ozone level exceeds 10 ppb in your laboratory.

Always use fresh Oligo aCGH Wash Buffer 1 and Oligo aCGH Wash Buffer 2 for each wash group (up to five slides).

The acetonitrile (dish #4) and Stabilization and Drying Solution (dish #5) below may be reused for washing up to 4 batches of 5 slides (total 20 slides) in one experiment. Do not pour the Stabilization and Drying Solution back in the bottle.

1 Completely fill slide-staining dish #1 with Oligo aCGH Wash Buffer 1 at room temperature.

2 Put a slide rack into slide-staining dish #2. Add a magnetic stir bar. Fill slide-staining dish #2 with enough Oligo aCGH Wash Buffer 1 at room temperature to cover the slide rack. Put this dish on a magnetic stir plate.

3 Put the prewarmed 1.5 L glass dish filled with water and containing slide-staining dish #3 on a magnetic stir plate with heating element. Fill the slide-staining dish #3 approximately three-fourths full with Oligo aCGH Wash Buffer 2 (warmed to 37 °C). Add a magnetic stir bar. Turn on the heating element and maintain temperature of Oligo aCGH Wash Buffer 2 at 37 °C; monitor using a thermometer.

4 In the fume hood, fill slide-staining dish #4 approximately three-fourths full with acetonitrile. Add a magnetic stir bar and put this dish on a magnetic stir plate.

5 In the fume hood, fill slide-staining dish #5 approximately three-fourths full with Stabilization and Drying Solution. Add a magnetic stir bar and put this dish on a magnetic stir plate.

6 Remove one hybridization chamber from incubator and resume rotation of the others. Record whether bubbles formed during hybridization, and if all bubbles are rotating freely.

7 Prepare the hybridization chamber disassembly.

a Put the hybridization chamber assembly on a flat surface and loosen the thumbscrew, turning counter-clockwise.

b Slide off the clamp assembly and remove the chamber cover.

c With gloved fingers, remove the array-gasket sandwich from the chamber base by lifting one end and then grasping in the middle of the long sides. Keep the microarray slide numeric barcode facing up as you quickly transfer the sandwich to slide-staining dish #1.

d Without letting go of the slides, submerge the array-gasket sandwich into slide-staining dish

#1 containing Oligo aCGH Wash Buffer 1.

8 With the sandwich completely submerged in Oligo aCGH Wash Buffer 1, pry the sandwich open from the barcode end only. Do this by slipping one of the blunt ends of the forceps between the slides and then gently twist the forceps to separate the slides. Let the gasket slide drop to the bottom of the staining dish. Remove the microarray slide, grasp it from the upper corners with thumb and forefinger, and quickly put into slide rack in the slide-staining dish #2 containing Oligo aCGH Wash Buffer 1 at room temperature. Minimize exposure of the slide to air. Touch only the barcode portion of the microarray slide or its edges!

9 Repeat step 6 through step 8 for up to four additional slides in the group. A maximum of five disassembly procedures yielding five microarray slides is advised at one time in order to facilitate uniform washing.

10 When all slides in the group are placed into the slide rack in slide-staining dish #2, stir using setting 4 for 5 minutes. Adjust the setting to get good but not vigorous mixing.

11 Transfer slide rack to slide-staining dish #3 containing Oligo aCGH Wash Buffer 2 at 37 °C, and stir using setting 4 for 1 minute.

12 Remove the slide rack from Oligo aCGH Wash Buffer 2 and tilt the rack slightly to minimize wash buffer carry-over. Quickly transfer the slide rack to slide-staining dish #4 containing acetonitrile, and stir using setting 4 for 10 seconds.

13 Transfer slide rack to slide-staining dish #5 filled with Stabilization and Drying Solution, and stir using setting 4 for 30 seconds.

14 Slowly remove the slide rack trying to minimize droplets on the slides. It should take 5 to 10 seconds to remove the slide rack.

15 Discard used Oligo aCGH Wash Buffer 1 and Oligo aCGH Wash Buffer 2.

16 Repeat step 1 through step 15 for the next group of five slides using fresh Oligo aCGH Wash Buffer 1 and Oligo aCGH Wash Buffer 2 prewarmed to 37 °C.

17 Immediately put the slides with Agilent barcode facing up in a slide holder with an ozone-barrier

slide cover on top of the array as shown in Figure 4 on page 62.

18 Scan slides immediately to minimize impact of environmental oxidants on signal intensities. If necessary, store slides in original slide boxes in a N2 purge box, in the dark.

19 Dispose of acetonitrile and Stabilization and Drying Solution as flammable solvents.

Step 4. Microarray Scanning using Agilent SureScan, C or B Scanner

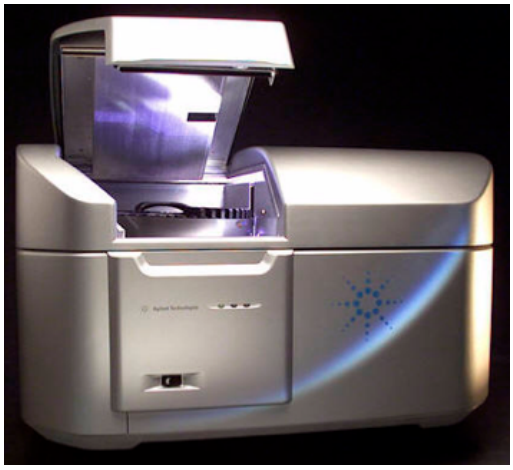

Figure 12: agilent scanner

Step 5. Data Extraction using Feature Extraction Software

5. RESULTS

5.1 Clinical results

From 1999 to 2011, 24 patients with histologically confirmed ONB were treated at Policlinico S. Matteo, University of Pavia, Ospedale di Circolo, University of Insubria, and Ospedali Civili di Brescia, University of Brescia.

Gender and age. Patients are 8 male and 16 females aged from 14 to 79 years old (mean 53,6 years).

Presenting Symptoms. 18 patients complained of nasal obstruction either alone or associated with other symptoms, epistaxis in 8, mucous rhinorrhea in 6, headache in 3. One patient was asymptomatic and the diagnosis was incidental.

Site of Origin. 18 tumours arose in the olfactory cleft and 6 arose in anterior ethmoid sinus.

Stage. According to the Kadish classification, disease in 4 patients was classified as stage A, 10 patients as stage B, and 10 patients as stage C. All the Kadish C patients in this series had intracranial extension with a focal invasion of the dura of the cribriform plate, with the exception of one patient with a massive dural involvment.

Hyams' Grading. Pathologic differentiation according to the Hyams' criteria revealed 6 Hyams' grading I, 13 Hyams' II, 5 Hyams' III tumours. Grade I and II tumours were considered as low-grade ON while grade III and IV tumours were considered as high-grade ON.

Treatment. 21/24 patients underwent an endoscopic resection with trasnasal craniectomy (ERTC), 3 patients underwent a cranioendoscopic resection due to he intracranial involvement laterally to the virtual plane passing the lamina papyracea.

23/24 patients underwent an adjuvant RT on the primary site of tumour, one patient refused postoperative radiotherapy. In 1 patient RT was administered in association with systemic chemotherapy postoperatively, due to the periorbital extension and the young age. The mean dosage administered was 56.1 6 5 SD Gy, with the technique previously described.

Intraoperative Margins. In 23/24 of these cases, surgical margins were free of disease, in only one

case with massive intracranial intradural involvement, extended laterally over the orbital roof, infiltration of the margins was observed. This patient underwent an andoscopic endonasal resection becasuse the old age and the comorbidities contraindicated the external approach (cranioendoscopic approach).

Local, Regional and Distant Recurrence

4/24 patients presented a local recurrence of disease, 3 patients presented a progression of the disease to the cervical nodes and 1 among these patients had distant metastasis.

Survival. All the patients are alive: 4/24 with disease and 20/24 free of disease. Follow-up ranged from 1 to 153 months (mean, 60 months), but in 6 patients, the follow-up is still too short (less than 3 years) to draw any conclusion. Every patient regained his or her normal daily activities with excellent quality of life. In Fig. 13 the disease-free interval of patients with ONB and neuroendocrine carcinoma is showed. The overall survival of all patients at 10 years was 100%. (Fig. 14)

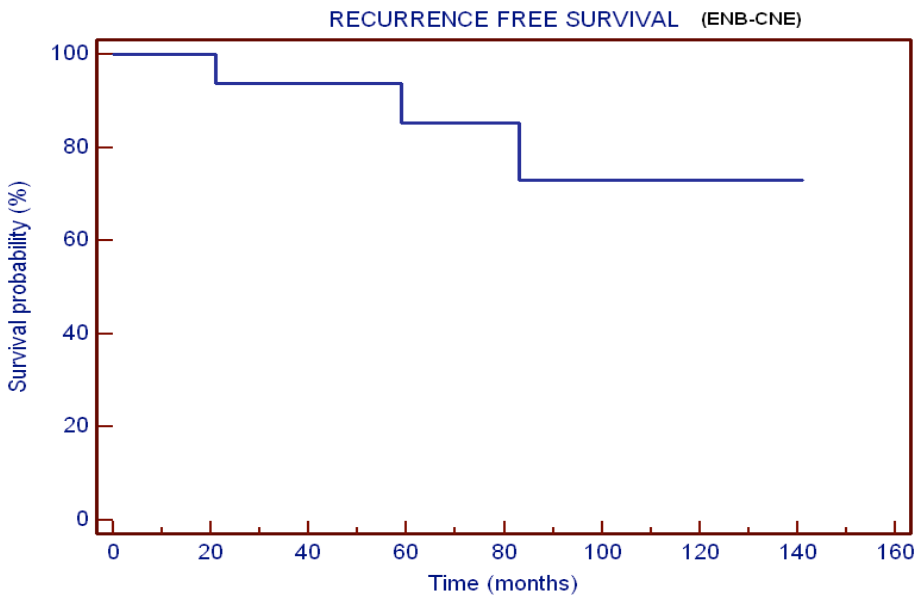

Figure 13: Recurrence free survival ONB and NEC

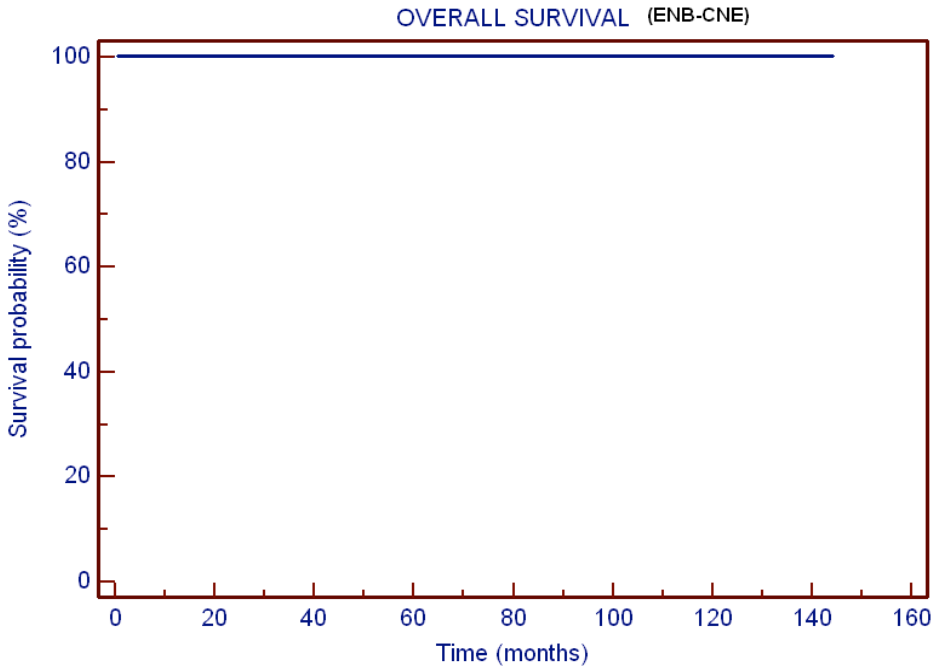

Figure 14: overall survival of ONB and NEC

5.2 Hystopatological results

The revaluation of morphological and immunophenotypic profile, with particular reference to the expression of cytokeratins, allowed to reclassify 3 of 24 patients with ONB in NEC.

morphological study

The olfactory neuroblastoma showed a low number of mitosis (counted in 10 fields at high magnification X400): on average 2 mitosis, with a variability between 0 and 6 mitoses; counts of MIB-1 (Ki-67) of 2000 neoplastic cells, showed a proliferative index of about 10%, with a range between 2% and 20%. In most cases, was not present angioinvasione and no tumour showed signs of neuroinvasione. In 7 patients bony structures invasion was present. Furthermore, only in 2 cases there were areas of necrosis.

In poorly differentiated neuroendocrine carcinomas mitotic counts for 10 HPF, was much higher (with an average value of 30 and with a variability of between 20 and 60 mitosis), the proliferative index MIB-1 (Ki-67, counted of 2000 cells) was equal to 46% with a variability between 20% and 80%.

In all cases it was evident the presence of necrosis, often with the characteristic appearance to "map". The angioinvasione, the neuroinvasione and infiltration of bone were present only in small part.

immunohistochemical study

In olfactory neuroblastoma staining for synaptophysin was present in most cases, as the immunoreactivity for chromogranin A. It was also observed the expression of S-100 protein, and not of cytokeratins.

While neuroendocrine carcinomas, cytokeratin AE1/AE3 was expressed in all carcinomas and there was no immunoreactivity for S100 protein.

This finding correlates well with the rate of recurrence of disease is different in patients with neuroendocrine carcinoma and ONB. In Fig. 13 is the disease-free interval of patients with ONB and neuroendocrine carcinoma.

Figures 15 and 16 show the disease-free interval of ONB and NEC after the pathologic reclassification. The figures show a recurrence earlier and more frequently in patients with neuroendocrine carcinoma compared to olfactory neuroblastoma.

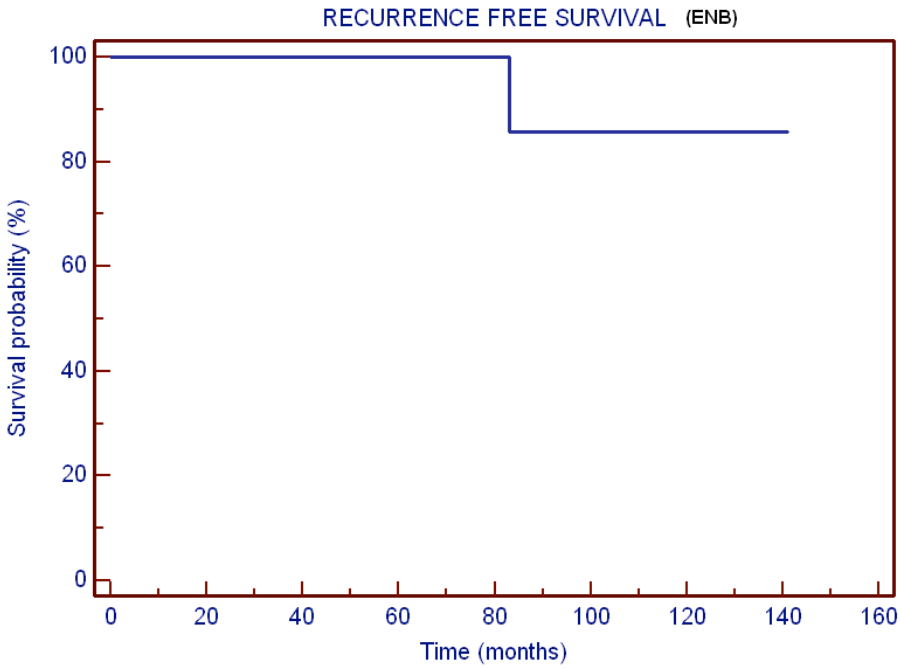

Figure 15: Recurrence free survival ONB

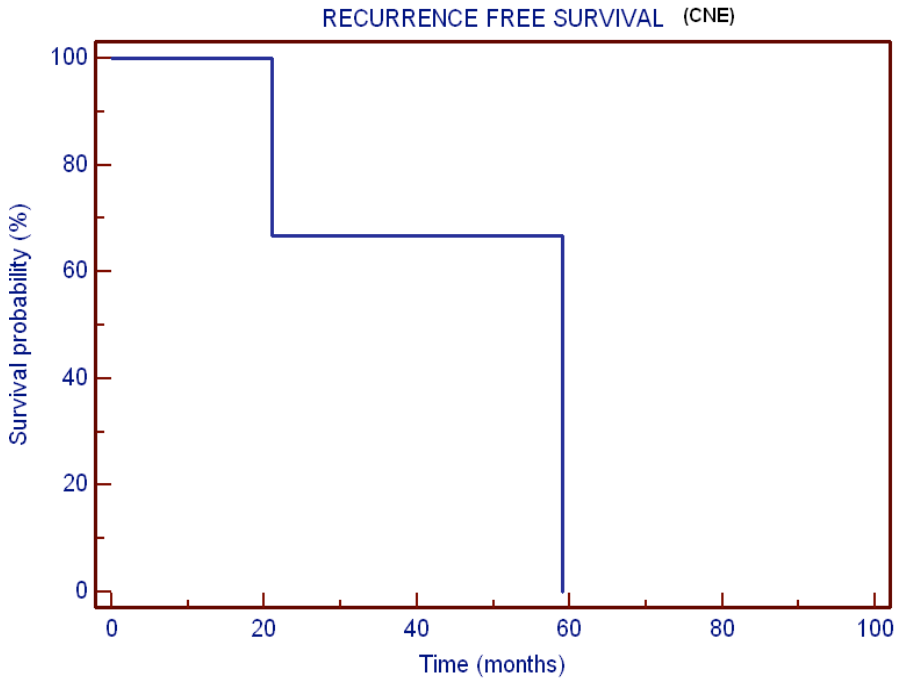

Figure 16: Recurrence free survival of NEC

5.3 a-CGH results

Array CGH was applied to study gene copy number alterations in 11 patients (10/11 with olfactory neuroblastoma and in 1/11 patient with NEC after the revision of the slides) (Table 9).

N.	Name	Sex	Histo	Hyms	Prim/rec	DNA
1	MG	M	ONB	II	P	DNA (FFPE)
					R	DNA (FFPE)
2	MC	F	NEC	III	P	DNA not quantifiable
					R	DNA (FFPE)
3	VI	M	ONB	II	P	DNA (fresh)
4	PM	M	ONB	II	P	DNA (FFPE)
5	DS	M	ONB	II	P	DNA (FFPE)
6	TI	F	ONB	II	P	DNA (FFPE)
7	PF	F	ONB	I	P	DNA (FFPE)
8	PD	F	ONB	II	P	DNA (fresh)
9	FL	M	ONB	II	P	DNA (FFPE)
10	GG	M	ONB	II	P	DNA (FFPE)
11	MG	F	ONB	III	P	DNA (FFPE)

Table 9: patients. In the table the initial of the patient name, the sex, the histophathological classification and the Hyams' grade, the recurrence, the DNA extraction. Abbreviation: ONB-olfactory neuroblastoma, NEC-neuroendocrine carcinoma, TP-primitive tumour, R-recurrence, FFPE-fixed and paraffin-embedded material.

The CGH Explorer software was used to analyze global frequencies of copy number change

A-CGH analysis of DNA has revealed amplifications and deletions showed in table n.10 and 11.

In table 10 amplificationts for each chromosome and for each patient are summarized and in table 11 deletions.

Pz\ch	1+	2+	5+	6+	7+	8+	9+	10+	11+	12+	13+	14+	15+	16+	17+	18+	19+	20+	21+	22+	X+	Y+
1-P		pq	pq	pq	pq		pq		pq		q12-13q31.1			pq	pq	pq	pq	pq			pq	
1-R		p	pq	pq	pq				pq				q			q		q			q	
		q12-q35																				
		q36.1-q36.3																				
2									pq			q	q			pq	p	pq				
3		p12-q12.1	pq		pq				pq		q	q	q	pq		pq	pq	pq	q	q	pq	
4			p13.3-p14.3	p21.1-p22.2	p22.1-pter				p15.4-pter			q32.1 1-qter		16p	17p	q22.1	19p	p13-pter	q22.1 1-qter	pq		
					q11.2 2-22.11				p11.12-p11.2						17q		9q	20q				
					q22.1				q12.2-q14.4													
									q23.1-qter													
5			pq	pq	pq				pq		13q	14	15	pq	pq	pq	pq	pq		pq	pq	Y
6	q32.1-q32.2	pq	pq	pq	pq				pq			14	15	pq	pq	pq	pq	pq		pq		
7																						
8			pq	pq	pq	p12-p21.1	pq		q	p	p	p	p	pq	pq	pq		pq		q		
9			pq	pq	pq				pq			q	q	pq	pq	pq	pq	pq		q	pq	y
10					p21.3-pter		p13.1-p13.3		p15.4-pter									pq				
					qcen-q21.11		q33.2-qter		q12.1-14.1													
					q22.1-q22.2				q22.3-qter													
11		pq	pq	pq	pq			pq	pq	pq	q	q	q	pq	pq		pq	pq		q		

Table 10: amplificated regions for patient and for chromosomes showed by the a-CGH

Pz\ch	1-	3-	4-	8-	9-	10-	11-	12-	13-	15-	21-	X-	Y-
1-TP	p31.1-p12												q
	q23.1-q25.1							q24.21					
1-R	p31.1-p12												
	q23.1-q25.1												Yq
2													
3													q
4	1 (complesso)	3 compl	pq	pq	9 compl	pq		12 compl	pq	pq	q21.1-q21.3	p11.4-21.3	
5	q31.1-q32.1	3pcen-p12.3		p23.1-p23.2									
		3q21-q26.2											
6													
7													
8													
9													
10	pcenp33	pq	pq	pq		pq	11p11.2-p12	p					
	q23.1-qter							qcen-q13.11					
								q14.1-q24.11			q21.1-q22.11		Y
11													

Table 11: loss regions for patients and for chromosomes showed by the a-CGH

The most frequent alterations involved the amplification of chromosoma 7, 11 and 20, which are presented in 80% of the patients. Alterations occurring in at least 60% of the cases are amplification of whole chromosoma 5, 16, 17, 18, 19, amplification of short arms of chromosome (p) 6 and amplification of long arms of chromosome (q) 14 and 22 (fig. 17 and 18).

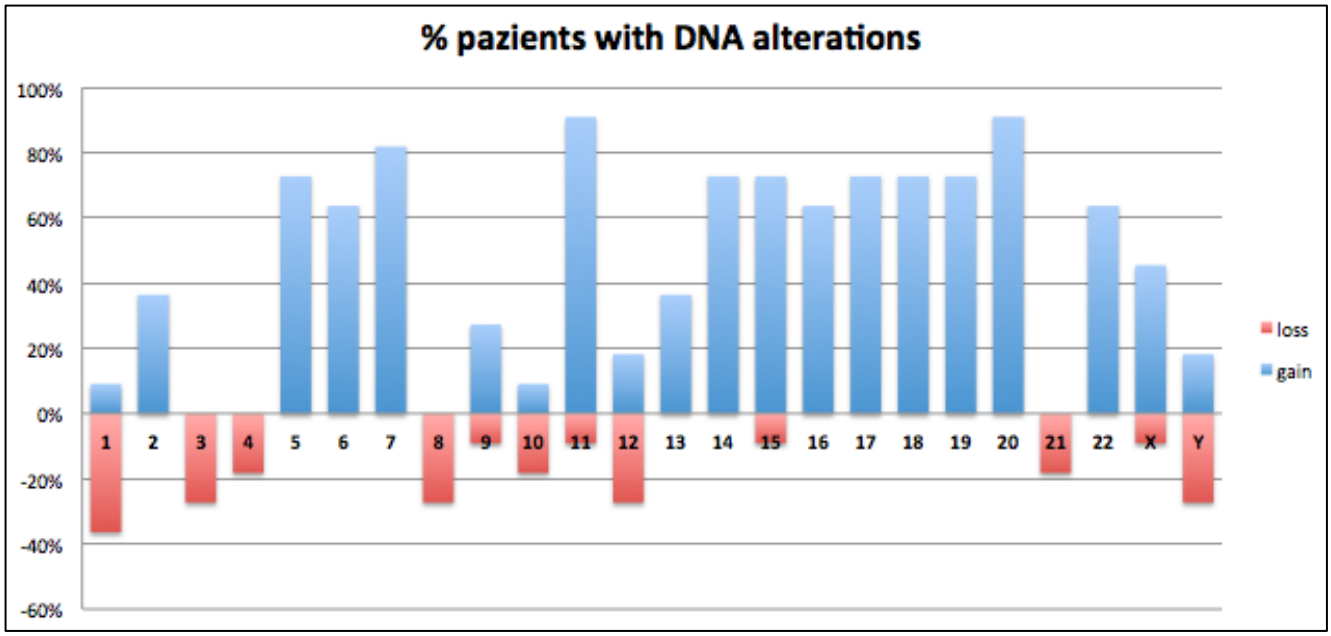

Figure 17: percentace of paients with DNA gain or loss for each chromosome. The Y axis shows the percentage of patients with gain or loss in chromosome. The X axis indicates the chromosome number.

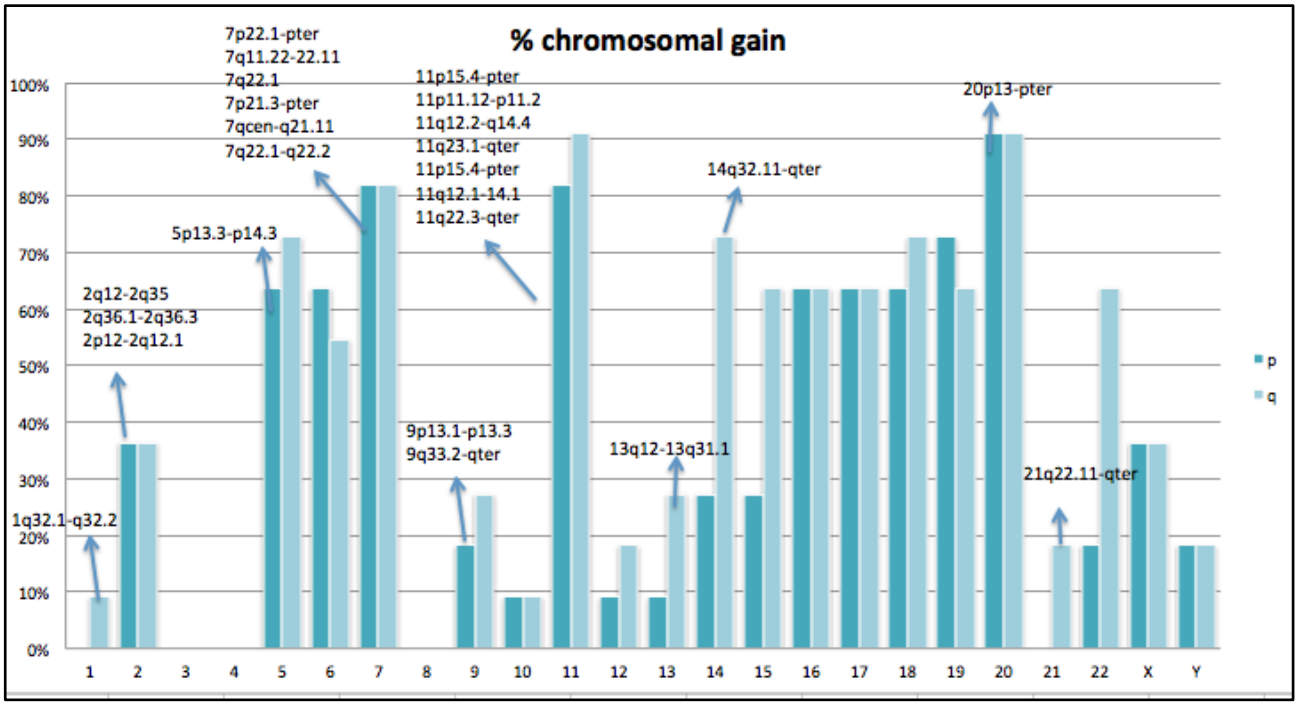

Figure 18: % of gain for each chromosome. The Y axis shows the percentage of patients. The x axis shows the short and long arm for each chromosome.

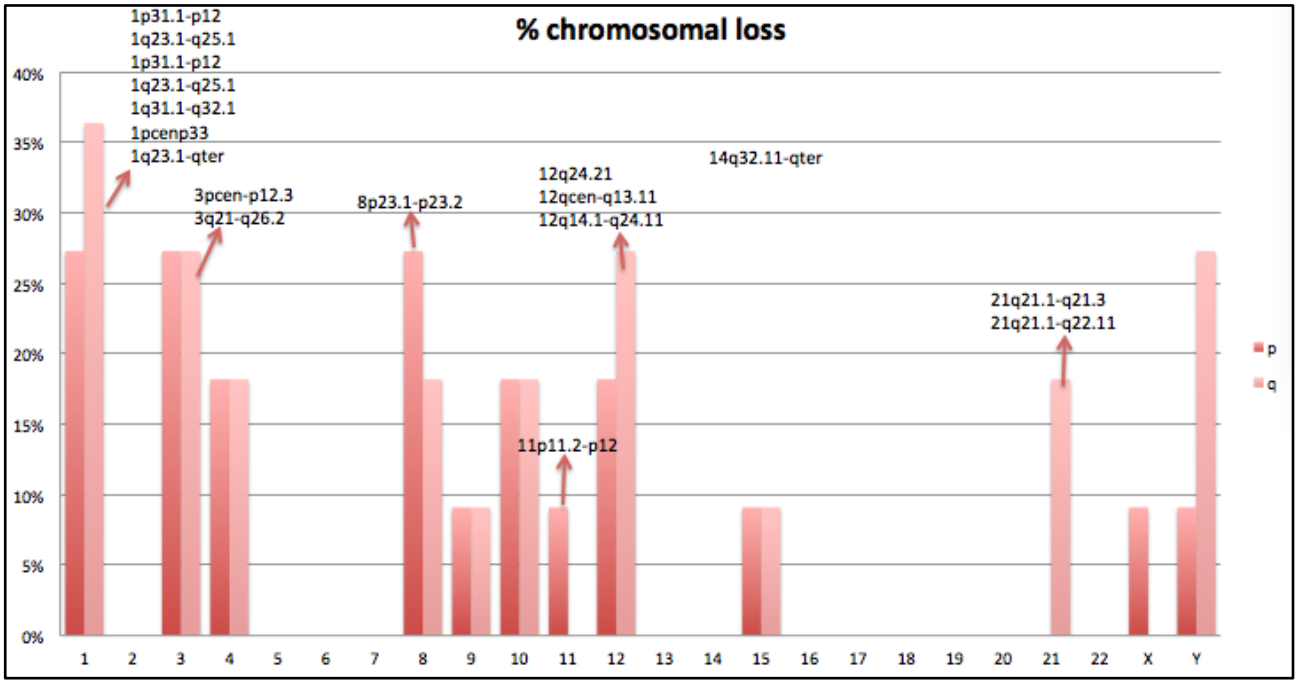

Figure 19: % of loss for each chromosome. The Y axis shows the percentage of patients . The x axis shows the short and long arm for each chromosome.

➢ Comparison with the literature

The results obtained with the technique of arrays were then compared with the results obtained from the work of Guled, the only literature where this technique is used. We analyzed the chromosomal regions in common between our patients and their patients. Table No. 19 shows the chromosomal alterations found in our cases and in the patients of the study of Guled with the same altered regions.

The long arms of chromosomes 13, 20, 22 and Xp present in our patients, are the most common in the study with which we have faced.

In addition to the duplicated regions, it was possible to identify monosomy of chromosome Y. This anomaly was found in all our male patients, and also has never been highlighted by previous studies.

By comparing the genetic profile of the NEC with the cases of ONB of the literature, we were able to identify two regions of chromosome 11 and duplication of chromosome 14 that are never described in cases of ONB in the literature. The only regions that overlap between the patient with neuroendocrine carcinoma and one case of the article by Guled is the duplication of chromosome 5q and chromosome 15. The patient who shared this region was one of the three patients who died in that study. It could be argued that even in the series by Guled olfactory neuroblastoma of the high-grade may be neuroendocrine carcinomas.

In accordance with this study, our patient had amplification of the 7q11.2 region that is implicated in other cancers such as prostate cancer, adenoidocistico cancer, squamous cell carcinoma and pancreatic endocrine carcinomas. A candidate gene located in this region, LIMK1 is a potential oncogene that contributes to cellular invasion.

Some alterations of small regions that were reported by approximately 50% of patients in the study Guled were also found in our patients. Not only small regions were altered, but also larger areas that included (gains of chromosome 5q, 13q, loss of chromosome 20 and Xp).

6. DISCUSSION

Olfactory neuroblastoma is an uncommon malignant neoplasm belived to arise from the olfactory epithelium. Since Berger and Luc first described olfactory neuroblastoma in 1924, more than 1025 cases of this tumour have been reported in the world literature, mostly as single or small case reports. More cases of olfactory neuroblastoma have been reported in the last 20 years but the low incidence does not permit to have clear data. In addition to the low incidence other factors contribute to the controversy associated with this neoplasm namely the tumour shows varying biological activity, ranging from indolent growth with patients surviving with known tumour for many years, to a highly aggressive neoplasm capable of rapid widespread metastasis with survival limited to a few months. Secondly, olfactory neuroblastoma is easily confused with other undifferentiated neoplasms of the nasal cavity.

Prognosis of ONB is strictly linked to histopathological grading. The grading system of Hyams is based on several tumour histological parameters from well differentiated to undifferentiate forms and has a good correlation to survival and relapse rate. Patients with low grade olfactory neuroblastoma has a better prognosis with a survival of more than 20 years (I and II grade 56%); while patients with neoplasm of higher grade disease has a very rapid progression, with a survival limitated to few months (III and IV grade 25%) (Bradley et al. 2003, Somenek et al. 2009).

The divergence between this two behaviour needs a better characterization of the patients with a worse prognosis. A revision of the report of the patients affected by olfactory neuroblastoma has been done in collaboration with the Department of Anatomical Pathology. A revision of all the histological slides was done and new histochimical techniques were used. Immunohistochemistry by using specific markers had differentiated 3 ONB in NEC. This histological variation well correlated to the clinical behaviour, namely the patients with NEC had a more aggressive course with a higrer rate of relapse (fig. 15 e 16).

The correct diagnosis permits the right treatment: infact the ONBs have as a gold standard surgery followed by radiotherapy, while NECs have only chemiotherapy as gold standard treatment.

Genetics of the tumour are very important to understand the cancerogenesis and besides have the aim to guide the therapeutics options. Because of the uncommon frequency of ONB, data of conventional and molecular cytogenetics are really limitated. The few data reported in literature try to show the pattern of ONB and are finalized to single out the genetic profile correlated to a worse prognosis.

Chromosomal Comparative Genomic Hybridization (CGH) is a molecular cytogenetic method for the detection of chromosomal imbalances (gain/losses) and it has been extensively used for studying copy number alterations in various cancer types since it was first described in 1992 (Kallioniemi et al. 1992). A-CGH is a new technique existing only in few centers in Italy. DNA from a test sample and normal reference sample are labelled differentially, using different fluorophores, and hybridized to several thousand probes. The probes are derived from most of the known genes and non-coding regions of the genome, printed on a glass slide. The fluorescence intensity of the test and of the reference DNA is then measured, to calculate the ratio between them and subsequently the copy number changes for a particular location in the genome.

Using this method, copy numbers changes at a level of 5-10 kilobases of DNA sequences can be detected.

Using this technique, our study has succeeded in defining a specific pattern of 8 ONB analyzing tumour DNA (7 primary tumours and 1 recurrence). This study is limited to 7 patients, since the extraction of DNA from fixed and paraffin-embedded material has not always given good results either for the amount of DNA used for the a-CGH or for the quality of the degraded DNA .

The extracted DNA, belongs to 6 patients with ONB (including 6 primary tumours and 1 recurrence) and a neuroendocrine carcinoma (primary and recurrent). The arrays were performed in only 8 DNA, as DNA extracted from the primary tumour of the NEC was not quantifiable, and the amplification did not yield enough. Initially we chose patients who had relapsed after our surgery to determine if the tumour was characterized by a more aggressive genetic profile.

The only patient with a recurrence of ONB had been treated with endoscopic endonasal technique

without the removal of the olfactory bulb and without postoperative RT. From the result of the array we noticed that there is a correlation between primary tumour and recurrence, although the number of genetic alterations detected is lower in the recurrence. This is the only patient with a recurrence of ONB: in this case, the surgical technique and the lack of RT may have influenced the prognosis which was favorable in all other cases. It was also the only patient with grade II Hyams who is relapsed.

The only patient grade III out of the seven patients analyzed, after review of the slides, was reclassified as a NEC. In fact, this patient (n. 2), despite the complete removal of technical understood the olfactory bulb, and despite the fact the patient had postoperative RT, it is still relapsed. In this case the worst prognosis is related to the pathology and not to the surgical technique with which the patient was treated. The DNA showed only a few alterations in common with ONB, perhaps some changes are not highlighted because the DNA was too degraded.

One patient, classified as grade I to Hyams, showed no genetic alterations; it could be due to the resolution of the technique.

In the literature there is only one study about ONB with a-CGH method performed by Guled et al. in 2008 and we are compared to that because it is the only one that has used the same method.

According to a further assertion of the study of Guled, the alterations of the long arms of chromosomes 13 and 20 are also present in our patients with ONB, it probably plays an important role in tumour progression. The gain of 20q has been associated with the progression of several cancers, such as lung cancer and pancreatic cancer (Guled 2008). In addition, gains and losses of 13q have showed an important role in various cancers, suggesting the existence of new oncogenes or oncosopressori in this region.

We also observed high frequency of chromosome 22 and Xp duplication. Such regions have been observed in previous studies (Bochmuhl 2004).

The monosomy of chromosome Y was found exclusively in our cases.

In addition Guled et al. in their work have defined the possible genes with a key role in the

progression of olfactory neuroblastoma. However, since the very large candidate regions, both in his and in our work, it is difficult to define the presence of genes actually involved in carcinogenesis.

Our patients had a number of small regions that deviate from the baseline, many of which overlap with regions known as the copy number variation (CNVs). In our study, given the high number of suspicious regions of CNVs, it is not possible to define which CNVs may be involved in tumour pathogenesis. The distinction between benign CNVs CNVs pathological and must therefore be carried out using a number of patients in large association studies.

This work also aims to emphasize the efficiency of a-CGH in the study of solid tumours. This method could be elected in the study of cancer, generally because it is difficult to obtain chromosome preparations from cultured tumour cells. In addition to the standard cytogenetic one could not get a picture cytogenetic satisfactory as it is known that tumours have a high degree chromosomal imbalances. Other methods such as CGH and multipainting conventional or FISH showed only gross and imbalances are not able to define abnormalities of small size, note that in the a-CGH has a resolution of ~ 8Kb.

It remains a very expensive technique, complex to implement and interpret, therefore, has a very limited use for now.

In conclusion these preliminary results, although obtained in only seven patients, demonstrated that the a-CGH is a tool of fundamental importance in the study of cytogenetic abnormalities in solid tumours.

The results obtained in our study, could contribute in the future to increase the evidence that genetic aberrations can clarify the pathogenic mechanism and have become a major clinical and therapeutic management dell'estesioneuroblastoma. Through a detailed understanding of genomic patterns, we could better define tumour aggressiveness and also find targeted therapeutic protocols.

A-CGH will require further analysis based on larger series to determine the role of the regions identified in ONB and to validate the results of our study.

Finally we want to emphasize that this study has been realized only through close collaboration between different departments: the ENT clinic of Varese, the Department of Pathology and the Department of Biology and Medical Genetics, Department of Clinical and Experimental medicine, who have made available to the excellence of their work. As the patients were treated with the most modern techniques of micro-invasive surgery, the tumour tissue was analyzed with the most advanced histochemical techniques and finally the genetic profile of the extracted DNA was characterized by the finest and most detailed molecular biology techniques.

7. REFERENCES

1. Barnes L, Eveson JW, Reichart P, Sidransky D. (Eds): World Health Organization Classification of Tumours. Pathology and Genetics of Head and Neck Tumours. IARC Press: Lyon 2005
2. Berger RL, Luc R: l´esthesioneuroepitheliome Olfactif. *Bull Assoc Franc Pour L´etude Cancer* 13 : 410-420, 1924.
3. Bockmühl U, You X, Pacyna-Gengelbach M, Arps H, Draf W, Petersen I. CGH pattern of esthesioneuroblastoma and their metastases. *Brain Pathol.* Apr;14(2):158-63, 2004.
4. Broich G, Pagliari A, Ottavini F: Esthesioneuroblastoma: A General Review of the Cases Published Since the Discovery of the Tumour in 1924. *Anticancer Research* 17: 2683-2706.
5. Broich G, Pagliari A, Ottaviani F. Esthesioneuroblastoma: a general review of the cases published since the discovery of the tumour in 1924. *Anticancer Res.* 1997;17(4A):2683-2706.
6. Bradley PJ, Jones NS, Robertson I. Diagnosis and management of esthesioneuroblastoma. Curr Opin Otolaryn- gol Head Neck Surg 2003;11:112–118.
7. Cakmak O, Ergin NT, Yilmazer C, Kayaselçuk F, Barutcu O. Endoscopic removal of esthesioneuroblastoma. Int J Pediatr Otorhinolaryngol. 2002 Jul 9;64(3):233-8.
8. Carter NP. Methods and strategies for analyzing copy number variation using DNA microarrays. Nat Genet. 2007 Jul;39(7 Suppl):S16-21.
9. Casiano RR, Numa WA, Falquez AM. Endoscopic resection of esthesioneuroblastoma. Am J Rhinol. 2001 Jul-Aug;15(4):271-9.
10. Castelnuovo P, Battaglia P, Locatelli D et al. Endonasal micro-endoscopic treatment of the malignant tumours of paranasal sinuses and anterior skull base. *Operative Techniques in Otolaryngology.* 17(3):152-167, 2006.
11. Castelnuovo P, Bignami M, Delù G, Battaglia P, Bignardi M, Dallan I: Endonasal endoscopic resection and radiotherapy in olfactory neuroblastoma: our experience. *Head & Neck* Sep;29(9):845-50, 2007.

12. Castelnuovo P: La dissezione anatomica endoscopica del distretto rino-sinusale – Il training anatomo-chirurgico per le tecniche di base della chirurgia endoscopica rino-sinusale. Editore Endo-Press, Tuttlingen, Germania, 2001.
13. Davis RE, Weissler MC: Esthesioneuroblastoma and Neck Metastasis. *Head & Neck* 14: 477-482, 1992.
14. Derdeyn CP, Moran CJ, Wippold FJ 2nd, Chason DP, Koby MB, Rodriguez F: MRI of Esthesioneuroblastoma. *JCAT* 18: 16-21, 1994.
15. Dulguerov P, Calcaterra M: Esthesioneuroblastoma: The UCLA Experience 1970-1990. *Laryngoscope* 102: 843-848, 1992.
16. Dulguerov P, Allal AS, Calcaterra TC. Esthesioneuroblastoma: a meta-analysis and review. Lancet Oncol 2001;2:683–690. [PubMed: 11902539
17. Eden BV, Debo RF, Larner JM, Kelly MD, Levine PA, Stewart FM, Cantrell RW, Constable WC, Esthesioneuroblastoma – Long Term Outcome and Patterns of Failure – The University of Virginia Experience. *Cancer* 73: 2556-2562, 1994.
18. Eich HT, Staar S, Micke O, Eich PD, Stützer H, Müller RP: Radiotherapy of Esthesioneuroblastoma. *Head and Neck* 49: 155-160, 2001.
19. Eriksen JG, Bastholt L, Krogdahl AS, Hansen O, Joergensen KE: Esthesioneuroblastoma: What is the Optimal Treatment? *Acta Oncologica* 39: 231-235, 2000.
20. Faragalla H, Weinreb I. Olfactory neuroblastoma: a review and update. Adv Anat Pathol 2009;16:322–331
21. Folbe A, Herzallah I, Duvvuri U, Bublik M, Sargi Z, Snyderman CH, Carrau R, Casiano R, Kassam AB, Morcos JJ. Endoscopic endonasal resection of esthesioneuroblastoma: a multicenter study. Am J Rhinol Allergy. 2009 Mar-Apr;23(2):238.
22. Ferlito A, Rinaldo A, Rhys-Evans PH. Contemporary clinical commentary: esthesioneuroblastoma: an update on management of the neck. Laryngoscope. 2003 Dec;113(12):2227.

23. Guled M, Myllykangas S, Frierson HF Jr, et al. Array comparative genomic hybridization analysis of olfactory neuroblastoma. Mod Pathol. 2008;21:770–778.
24. Holland H, Koschny R, Krupp W, Meixensberger J, Bauer M, Kirsten H, Ahnert P. Comprehensive cytogenetic characterization of an esthesioneuroblastoma. Cancer Genet Cytogenet. 2007 Mar;173(2):89-96.
25. Hyams VJ: Tumours of the Upper Respiratoy Tract and Ear. In: Hyams VJ, Batsakis JG, Michaels L, eds. *Atlas of Tumour Pathology.* 2nd series, Fascicle 25. Washington, DC: Armed Forces Institute of Pathology, 1988, p. 240-248.
26. Hyams VJ, Batsakis JG, Michaels L. Tumours of the upper respiratory tract and ear. Armed Forces Institute of Pathology Fascicles, 2nd series. Washington : American Registry of Pathology Press; 1988.
27. Jethanamest D, Morris LG, Sikora AG, Kutler DI. Esthesioneuroblastoma: a population-based analysis of survival and prognostic factors. Arch Otolaryngol Head Neck Surg. 2007 Mar;133(3):276-80.
28. Jiang GY, Li FC, Chen WK, Liu AM, Cai WQ. Therapy and prognosis of intracranial invasive olfactory neuroblastoma. Otolaryngol Head Neck Surg. 2011 Dec;145(6):951-5.
29. Kadish S, Goodman M, Wang CC: Olfactory Neuroblastoma, a Clinical Analysis of 17 Cases. *Cancer* 37: 1571-1576, 1976.
30. Kallioniemi A, Kallioniemi OP, Sudar D, et al. Comparative genomic hybridization for molecular cytogenetic analysis of solid tumours. Science 1992; 258: 818-21
31. Kareimo KJA, Jekunen AP, Kestilä MS, Ramsay HA: Imaging of Olfactory Neuroblastoma – an Analysis of 17 Cases. *Auris Nasus Larynx* 25: 173-179, 1998.
32. Ketcham AS, Wilkins RH, Van Buren JM, Smith RR: A Combined Intracranial Facial Approach to the Paranasal Sinuses. *Am J Surg* 166: 698-703, 1963.
33. Koka VN, Julieron M, Bourhis J, Janot F, Le Ridant AM, Marandas P, Luboinski B, Schwaab G. Aesthesioneuroblastoma. J Laryngol Otol. 1998 Jul;112(7):628-33.

34. Levine PA, Debo RF, Meredith SD, Jane JA, Constable WC, Cantrell RW: Craniofacial Resection at the University of Virginia (1976-1992): Survival Analysis *Head Neck* 16: 574-577, 1994.
35. Levine PA, Gallagher R, Cantrell RW: Esthesioneuroblastoma: Reflections of a 21-Year Experience. *Laryngoscope* 109: 1539-1543, 1999.
36. Levine PA, McLean WC, Cantrell RW: Esthesioneuroblastoma: the University of Virginia Experience 1960-1985. *Laryngoscope* 96: 742-746, 1986.
37. Levine PA, Scher RL, Jane JA, Persing JA, Newman SA, Miller J, Cantrell RW: The Craniofacial Resection - Eleven-Year Experience at the University of Virginia: Problems and Solutions. *Otolaryngol Head Neck Surg* 101: 665-669, 1989.
38. Locatelli D, Castelnuovo P, Santi L, Cerniglia M, Maghnie M, Infuso L: Endoscopic Approaches to the Cranial Base: Perspectives and Realities. *Child`s Nerv Syst* 16: 686-691, 2000.
39. Lund VJ, Howard D, Wei W, Spittle M. Olfactory neuroblastoma: past, present, and future? Laryngoscope 2003;113:502–507. [PubMed: 12616204
40. Lund VJ, Stammberger H, Nicolai P, Castelnuovo P, Beale T, Beham A, Bernal-Sprekelsen M, Braun H, Cappabianca P, Carrau R, Clarici G, Draf W, Esposito F, Fernandez-Miranda J, Fokkens WJ, Gardner P, Gellner V, Hellquist H, Hermann P, Hosemann W, Howard D, Jones N, Jorissen M, Kassam A, Kelly D, Kurschel-Lackner S, Leong S, McLaughlin N, Maroldi R, Minovi A, Mokry M, Onerci M, Ong YK, Prevedello D, Saleh H, Sehti DS, Simmen D, Snyderman C, Solares A, Spittle M, Stamm A, Tomazic P, Trimarchi M, Unger F, Wormald PJ, Zanation A. European position paper on endoscopic management of tumours of the nose, paranasal sinuses and skull base. Rhinology 2010;48(Suppl 22):46–51.
41. Mc Elroy EA, Buckner JC, Lewis JE: Chemotherapy for Advanced Esthesioneuroblastoma: The Mayo Clinic Experience. *Neurosurgery* 42: 1023-1028, 1998.
42. Miyamoto RC, Gleich LL, Biddiger PW, Gluckman JL: Esthesioneuroblastoma and Sinonasal Undifferentiated Carcinoma: Impact of Histological Grading and Clincal Staging on Survival and Prognosis. *Laryngoscope* 110: 1262-1265, 2000.

43. Morita A, Ebersold MJ, Olsen KD, Foote RL, Lewis JE, Lynn MQ: Esthesioneuroblastoma: Prognosis and Management. *Neurosurgery* 32: 706-715, 1993.

44. Nicolai P, Battaglia P, Bignami M, Bolzoni Villaret A, Delù G, Tarek K, Lombardi D, Castelnuovo P. Endoscopic surgery for malignant tumours of the sinonasal tract and adjacent skull base: a 10-year experience. *Am J Rhinol.* May-Jun;22(3):308-16, 2008.

45. Olsen KD, DeSanto LW: Olfactory Neuroblastoma – Biologic and Clinical Behavior. *Arch Otolaryngol* 109: 797-802, 1983.

46. Pickuth D, Heywang-Köbrunner SH: Imaging of Recurrent Esthesioneuroblastoma. *The British Journal of Radiology* 72: 1052-1057, 1999.

47. Resto VA, Eisele DW, Forastiere A, Zahurak M, Lee DJ, Westra WH: Esthesioneuroblastoma: the Johns Hopkins Experience. *Head & Neck* 22: 550-558, 2000.

48. Riazimand SH, Brieger J, Jacob R, et al. Analysis of cytogenetic aberrations in esthesioneuroblastomas by comparative genomic hybridization. Cancer Genet Cytogenet. 2002; 136:53–57

49. Esthesioneuroblastoma and cervical lymph node metastases: clinical and therapeutic implications. Rinaldo A, Ferlito A, Shaha AR, Wei WI, Lund VJ. Acta Otolaryngol. 2002 Mar;122(2):215-21.

50. Schmidt JL, Zarbo RJ, Clark JL: Olfactory Neuroblastoma: Clinicopathologic and Immunohistochemical Characterization of Four Representative Cases. *Laryngoscope* 100: 1052-1058, 1990.

51. Schuster JJ, Phillips CD, Levine PA. MR of esthesioneuroblastoma (olfactory neuroblastoma) and appearance after craniofacial resection. AJNR Am J Neuroradiol. 1994 Jun;15(6):1169-77.

52. Schwaab G, Micheau C, Pacheco L, Domenge C, Le Gouillou C, Marandas P, Richard JM, Wibault P: Olfactory Esthesioneuroma: a Report of 40 Cases. *Laryngoscope* 98:872-876, 1988.

53. Sheehan JM, Sheehan JP, Jane JA, Polin RS: Chemotherapy for Esthesioneuroblastomas. *Neurosurg Clin N Am* 11: 693-701, 2000.

54. Simon C, Touissaint B, Coffinet L. Tumeurs malignes des cavités nasales et paranasales. Encycl Méd Chir (Elsevier, Paris), Oto-rhino-laryngologie, 20-405-A-10, 1997, 19 p.
55. Simon C, Toussaint B, Coffinet L : Tumeurs malignes des cavités nasales et paranasales. Encycl Méd Chir (Elsevier, Paris), Oto-rhino-laryngologie, 20-405-A-10, 1997, 19 p.
56. Som PM, Lidov M, Brandwein M, Catalano P, Biller HF. Sinonasal esthesioneuroblastoma with intracranial extension: marginal tumor cysts as a diagnostic MR finding. AJNR Am J Neuroradiol. 1994 Aug;15(7):1259-62.
57. Somenek M, Shera NC, Petruzzelli GJ, Origitano TC: Estesioneuroblastoma. *Oncology* 2009
58. Stammberger H, Anderhuber W, Walch C, Papaefthymiou G: Possibilities and Limitations of Endoscopic Management of Nasal and Paranasal Sinus Malignancies. *Acta oto-rhino-laryngoloica belg* 53: 199-205, 1999.
59. Stammberger H: Diagnosi Endoscopica e Radiologica. In Stammberger H: Chirurgia Endoscopica Funzionale dei Seni Paranasali. Torino, Centro Scientifico Editore, 1992.
60. Szymas J, Wolf G, Kowalczyk D, Nowak S, Petersen I: Olfactory Neuroblastoma: Detection of Genomic Imbalances by Comparative Genomic Hybridization. *Acta Neurochir (Wien)* 139: 839-844.
61. Thompson LD. Olfactory neuroblastoma. Head Neck Pathol. 2009 Sep;3(3):252-9.
62. Unger F, Walch C, Stammberger H, Papaefthymiou G, Haselsberger K, Pendl G: Olfactory Neuroblastoma (Esthesioneuroblastoma): Report of Six Cases Treated by a Novel Combination of Endoscopic Surgery and Radiosurgery. *Minim Invasive Neurosurg* 44: 79-84, 2001.
63. Walch C, Stammerger H, Anderhuber W, Unger F, Köle W, Feichtinger K: The Minimally Invasive Approach to Olfactory Neuroblastoma: Combined Endoscopic and Stereotactic Treatment. *Laryngoscope* 110: 635-640, 2000.
64. Woodhead P, Lloyd GA. Olfactory neuroblastoma: imaging by magnetic resonance, CT and conventional techniques. Clin Otolaryngol Allied Sci. 1988 Oct;13(5):387-94.